

**DEEP-TOW STUDY OF MAGNETIC ANOMALIES IN THE PACIFIC
JURASSIC QUIET ZONE**

A Thesis

by

MASAKO TOMINAGA

Submitted to the Office of Graduate Studies of
Texas A&M University
in partial fulfillment of the requirements for the degree of

MASTER OF SCIENCE

August 2005

Major Subject: Oceanography

**DEEP-TOW STUDY OF MAGNETIC ANOMALIES IN THE PACIFIC
JURASSIC QUIET ZONE**

A Thesis

by

MASAKO TOMINAGA

Submitted to the Office of Graduate Studies of
Texas A&M University
in partial fulfillment of the requirements for the degree of

MASTER OF SCIENCE

Approved by:

Chair of Committee,	William W. Sager
Committee Members,	P. Jeff Fox
	Thomas W. C. Hilde
Head of Department,	Wilford D. Gardner

August 2005

Major Subject: Oceanography

ABSTRACT

Deep-tow Study of Magnetic Anomalies in the Pacific Jurassic Quiet Zone.

(August 2005)

Masako Tominaga, B.E., Waseda University

Chair of Advisory Committee: Dr. William W. Sager

The Jurassic Quiet Zone (JQZ) is a region of low amplitude, difficult-to-correlate magnetic anomalies located over Jurassic oceanic crust. We collected 1200 km of new deep-tow magnetic anomaly profiles over the Pacific JQZ that complement 2 deep-tow profiles reported in Sager *et al.* (1998). Our primary goals were to extend the correlation of deep-tow magnetic anomalies farther back in time, to evaluate the correlatability and repeatability of anomalies, and to refine the Jurassic geomagnetic polarity reversal time scale (GPTS). Correlations of anomalies were excellent over M34 and over supposedly older seafloor to the south of ODP Site 801. In contrast, the correlation in the region between M34 and Site 801 was difficult. Using anomaly correlation models, we made magnetic polarity block models to establish a revised Jurassic GPTS extending until 169.4 Ma. Age calibration was accomplished with radiometric dates from two ODP holes. Systematic changes in anomaly amplitudes occur along the survey lines with the amplitudes decreasing backward in time and then increasing again in the oldest part of survey area. The zone of the most difficult to correlate anomalies corresponds to a period of ~4 m.y. that appears to have an abrupt end. This low amplitude zone suggests unusual magnetic behavior during the Jurassic. It has been said that many of the larger anomalies

are likely caused by changes in polarity, whereas smaller anomalies may be intensity fluctuations. Although it is impossible to identify which anomalies are caused by reversals and which are not, magnetization structures observed in ODP Hole 801C suggest that many of the smallest anomalies, particularly around Hole 801C indicate polarity reversals. We concluded that (1) the new data demonstrates repeatability and correlatability of the JQZ magnetic anomalies implying that they are seafloor spreading lineations and (2) good correlations made new GPTS models extending back to 169.4 Ma; and (3) the origin of the JQZ may be a combination of rapid polarity reversals in the Jurassic low magnetic dipole field and closely spaced, tilted magnetization structure in the oceanic crust.

ACKNOWLEDGMENTS

I would like to thank my advisor, Dr. William W. Sager, and committee members, Dr. Thomas W. C. Hilde and Dr. P. Jeff Fox for their support and guidance throughout the process of completing my thesis. Their understanding of my works and scientific goals have encouraged my continued study. I am especially happy to have Will as my supervisor. Whenever I saw thick clouds ahead of me, he always offered considerate and professional advice to help me clear those. I also would like to specially thank: N. Abe, M. Aruga, A. Delacour, G. De la torre, S. Drew, “Nobu” Eguchi, J. Escartin, N. S. Fucker, T. Fujikawa, E. Fujisawa, S. Hang, A. C. Harris, B. Ildefonse, Y. Ito, H. P. Johnson, K. Kunimatsu, A. “Kotani” Kashima, A. J. Lamarche, C. F. Leahy III, D. S. Maddox, O. U. Mason, K. Michibayashi, N. Morita, “Yas” Ohara, A. Ogino, K. A. Roberts, “Sunny” Saito, “Aya” Sasahara, S. Tavernpanich, M. A. Tivey, C. M. Williams, R. M. Wheatley, M. S. Yeager, N. Yukitomo, X. Zhao, and Yayoi, Shozo, Yosuke, and Dishko Tominaga. Without these people, I could not reach today.

TABLE OF CONTENTS

	Page
ABSTRACT	iii
ACKNOWLEDGMENTS.....	v
TABLE OF CONTENTS	vi
LIST OF FIGURES.....	viii
INTRODUCTION.....	1
GEOLOGICAL BACKGROUND	4
DATA AND METHODS.....	7
1. Data Collection.....	7
2. Magnetic Data Processing.....	8
3. Correlation Models.....	9
4. Magnetic Polarity Block Model	14
5. Composite Model	16
6. Age Calibration Model.....	16
RESULTS.....	18
1. Correlation Model	18
2. Magnetic and Composite Model	19
3. Age Calibration	27
DISCUSSION	31
1. Correlation.....	31
2. Reversal Models.....	32
3. Correlation Between Our Models and Hole 801C Data.....	35
4. Implications for the Origin of the JQZ.....	38
CONCLUSIONS	43
REFERENCES.....	45

	Page
APPENDIX A	51
VITA	56

LIST OF FIGURES

FIGURE	Page
1 Survey area and regional bathymetry.....	5
2 Correlation of magnetic anomalies among lines 5-11, 5-12, and 5-13 in m34 survey area	10
3 Correlation of magnetic anomalies among lines 3-9, 2-1, 2-3, 3-4, 1, 2-5, and 2-7 in H801C survey area	11
4 Correlation of magnetic anomalies between lines 1 and 3-9 in the SOUTH survey area	12
5 Correlation of magnetic anomalies from Sager <i>et al.</i> (1998) and this study in the NORTH survey area	13
6 Correlation of magnetic anomalies among lines 5, 92-1, 4-1, 3-9, 3-6, and 92-2 in NORTH survey area.....	20
7 Composite model of magnetic polarity block model established in study of Sager <i>et al.</i> (1998, 92- composite model) and this study.	23
8 Composite magnetic polarity block model of the deep-tow profiles around Hole 801C	24
9 Composite magnetic polarity block model of the deep-tow magnetic profiles of the SOUTH survey area.....	25

FIGURE	Page
10 Power spectra of two segments of line 4-1	26
11 Age-calibration using two absolute ages from ODP sites	28
12 Composite magnetic polarity block model at mid-water level upward continued magnetic profiles.	29
13 Deep-tow and mid-water magnetic polarity model from this study compared with that of <i>Handshumacher et al.</i> (1988) and <i>Sager et al.</i> (1998).	30
14 Calculated anomaly intensities with various polarity widths.....	42

INTRODUCTION

The Jurassic period was a time of unusual geomagnetic behavior. Magnetic anomalies over seafloor of this age are small and difficult-to-correlate. [e.g. Larson and Chase, 1972; Larson and Pitman, 1972; Hayes and Rabinowitz, 1975; Barrett and Keen, 1976]. Because of this character, some have suggested that the Jurassic geomagnetic field was ‘quiet’ (i.e., non-reversing). Although the “Cretaceous Quiet Zone” has been recognized as a true polarity superchron, during which the geomagnetic field was in a nearly constant normal polarity state for ~ 35 Myr [e.g. Helsley and Steiner, 1969; Gradstein *et al.*, 1995; Cande and Kent, 1992a], the origin of the Jurassic Quiet Zone (JQZ) appears different. The JQZ is known from middle to Late Jurassic age seafloor in both Pacific and Atlantic oceans where the magnetic lineations are indistinct because of the reduction of anomaly amplitude to the point of incoherence. Contemporaneous land magnetostratigraphic data contain many geomagnetic field reversals [Steiner, 1980; Ogg *et al.*, 1984; Steiner *et al.*, 1985; Steiner *et al.*, 1987; Ogg *et al.*, 1991; Ogg and Gutowski, 1995], suggesting that the JQZ is not a period of constant polarity and that many of the small anomalies result from magnetic reversals [Cande *et al.*, 1978].

Over the years, the JQZ was pushed farther back in time as new correlatable anomalies were recognized deeper in the anomalous zone [e.g. Larson and Hilde, 1975; Cande *et al.*, 1978; Sager *et al.*, 1998]. Although M29 is the oldest anomaly accepted in most polarity reversal time scales, aeromagnetic and deep-tow magnetic data show many

This thesis follows the style of *Journal of Geophysical Research*.

older anomalies. The older anomalies are apparent in these data because they allow better separation of external magnetic variations relative to crustal anomalies [e.g. Handschumacher *et al.*, 1988; Sager *et al.*, 1998]. External field noise is particularly troublesome in the western Pacific JQZ, because in this area the external variations are large and often have similar wavelengths to crustal anomalies at typical ship speeds. With the aeromagnetic data, aircraft speed causes the wavelengths of external field variations, such as the diurnal effect, to be much wider than crustal anomalies, which is less confounding. Handshumacher *et al.* (1988) showed the existence of pre-M29 magnetic lineations using aeromagnetic data. Alternatively, deep tow data greatly increase the amplitude of crustal anomalies whereas the external field variations remain the nearly same. Data from a deep-tow magnetometer show the existence of many small correlatable anomalies back to the middle Jurassic in the Pacific JQZ [Sager *et al.*, 1998].

Understanding the nature, age, and even existence of the JQZ is of fundamental importance to wide range of geomagnetic studies. Its unique, low amplitude of magnetic anomalies invoke debates about how the Jurassic magnetic field operated. Whether such anomalies represent actual geomagnetic reversals or paleomagnetic field fluctuations changes interpretation of the GPTS and reversal rates, which may have been higher than at any time in recorded geomagnetic history [e.g. Cande and Kent, 1992a, 1992b; Sager *et al.*, 1998; Roser *et al.*, 2002; Bowles *et al.*, 2003].

Using a deep-tow magnetometer, Sager *et al.* (1998) investigated the western Pacific JQZ in the Pigafetta Basin, where the Jurassic crust was cored at Ocean Drilling

Program (ODP) Hole 801C. This site has highest resolution record for the JQZ studies because of its rapid spreading on Pacific-Izanagi Ridge [Nakanishi *et al.*, 1992]. The study was limited by having only two parallel deep tow profiles, which did not allow for a convincing test of repeatability at the oldest and of the deep-tow profiles. That study included a region of low amplitude anomalies for which correlations were tenuous. Furthermore, the deep-tow lines were not extended to either Hole 801C nor Rough-Smooth boundary that is supposed to be the end of the small anomaly sequence [Handschumacher *et al.*, 1988]. In this study, we specifically wanted to test anomaly repeatability by collecting multiple lines at certain locations. We also wanted to extend survey area to Hole 801C and the Rough-Smooth boundary.

Our primary goal was to make a combined correlation of new data and previous magnetic profiles to gain insight of the detailed features of the JQZ magnetic anomalies. The new data were also used to refine the magnetic polarity reversal model. Furthermore, new age data from Hole 801C, located in the study area, suggested that a recalibration of the Jurassic Geomagnetic Polarity Time Scale (GPTS) is in order [Koppers *et al.*, 2003a].

GEOLOGICAL BACKGROUND

JQZ studies using magnetic lineations from the seafloor have been carried out over similar age oceanic lithosphere in several regions: the western Pacific [e.g. Cande *et al.*, 1978; Handschmacher *et al.*, 1988; Sager *et al.*, 1998], the northwest Atlantic off the Nova Scotia margin [Barrett and Keen, 1976], and the eastern Atlantic off the Moroccan margin [e.g. Hayes and Rabinowitz, 1975; Roser *et al.*, 2002]. In the western Pacific, the sediment thickness is small, usually only several hundred meters over abyssal seafloor, allowing a deep-tow magnetometer to be close to the source layer. In addition, fast spreading rates make it possible to obtain high resolution of the anomalies. In contrast, in both the northwest and eastern Atlantic, sediment thickness of the continental margins increases the distance between the Jurassic oceanic crust and the magnetometer, lessening resolution. Furthermore, slower spreading rates in the Atlantic reduces the resolution of magnetic anomalies.

Our study area, the Pigafetta Basin, is located within the Marcus-Wake seamounts in the western Pacific, approximately 500 – 1000 km east of the northern Marianas Trench (Figure 1). Typical depths of the seafloor in Pigafetta Basin are about 6000 m, with several hundred meters of abyssal pelagic sediment [Bryant and Bennett, 1988; Lancelot *et al.*, 1990; Abrams *et al.*, 1993]. The oceanic lithosphere was originally formed at the NE-trending Pacific-Izanagi Ridge during the Jurassic [Nakanishi *et al.*, 1992]. Paleomagnetic studies at ODP Sites 800 and 801 indicate that the Pigafetta Basin

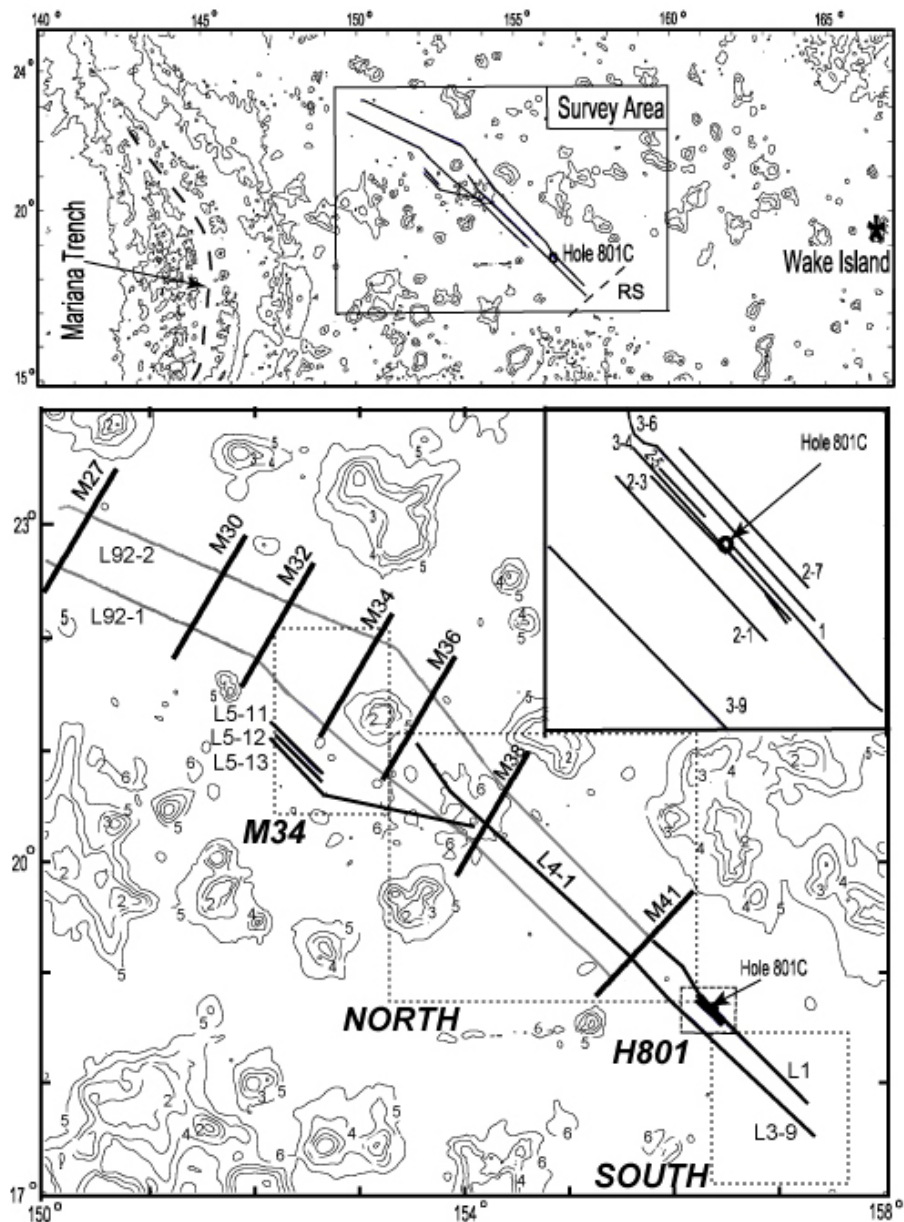


Figure 1. Survey area and regional bathymetry. Gray lines are ship tracks from Sager *et al.* (1998). Black lines are ship tracks from *R/V Thomas. G. Thompson* cruise (TN152, 2002-2003). Black bold lines are magnetic lineations suggested by Sager *et al.* (1998). Dotted squares are regional survey areas indicated in text.

lithosphere was formed slightly south of equator, then moved northward to its current location [Larson *et al.*, 1992]. The most significant post-Jurassic geologic event that occurred in the basin was intraplate volcanism during Early and middle Cretaceous, causing the eruption of several plateaus, numerous seamounts, and massive sills [Schlanger *et al.*, 1981, Koppers *et al.*, 2003b]. One might be concerned that such volcanism destroyed the prior magnetic signatures on the oceanic lithosphere; however, various studies have documented correlatable Jurassic and Early Cretaceous magnetic lineations in this region [e.g. Larson and Schlanger, 1981; Nakanishi *et al.*, 1992; Channel *et al.*, 1995]. Several factors are thought to explain the survival of pre-Cretaceous anomalies: (1) volcanic source vents were narrow, and the sills mainly intruded the sediment column, and (2) uniformly magnetized Cretaceous basalts would produce a magnetic anomaly only at its edges [Larson and Schlanger, 1981].

ODP Leg 129 (1989-1990) and Leg 185 (1999) succeeded in penetrating 474m into the Jurassic oceanic crust at Hole 801C [Lancelot *et al.*, 1990; Plank *et al.*, 2000]. The results of downhole magnetic measurements showed six polarities in the superimposed extrusive volcanic flows at Hole 801C [Plank *et al.*, 2000; Tivey *et al.*, 2005]. Also, paleomagnetic study of basalt section of Hole 801C by Steiner (2001) shows similar polarity reversals. $^{40}\text{Ar}/^{39}\text{Ar}$ radiometric dating was carried out to determine ages of the flow sequences. The oldest Jurassic basement is 167.4 ± 1.7 Ma, overlain by approximately 50 m of off-axis alkali basalts layer with any age of 160.1 ± 0.6 Ma [Koppers *et al.*, 2003a].

DATA AND METHODS

1. Data Collection

We used the data collected by R/V *Thomas Washington* (TUNE08WT) in 1992 [Sager *et al.*, 1998], and by R/V *Thomas G. Thompson* (TN152) in 2002-2003. During cruise of TUNE08WT, a three-axis deep-tow fluxgate magnetometer was towed at approximately \sim 1000 m above the seafloor at an average speed of 2.1- 2.5 kt (1.1- 1.3 ms^{-1}). During the TN152 cruise, a three-axis fluxgate magnetometer was placed on the deep-tow DSL-120 side-scan sonar and towed 100 m above the seafloor at an average speed of 1.2 kt (0.56 ms^{-1}). The magnetometer was towed close to the seafloor to amplify the crustal magnetic signals increasing the signal-to-noise ratio and mitigating the attenuation due to separation of source and sensor. Track lines were chosen to avoid seamounts and for orientation nearly perpendicular to the magnetic lineations identified in Sager *et al.* (1998) (Figure A-1). Three closely-spaced, subparallel lines are located over the extension of M34 (Line 5-11, -12, and -13), a well-defined anomaly from the previous survey (Figure 1). In the region of Hole 801C, seven subparallel lines were collected in small area around the drill site (Lines 1, 2-1, -3, -5, and -7, 3-4, -6, and -9) (Figure 1). In the southern part of the study area, two subparallel lines extend from Hole 801C to the Rough-Smooth boundary (Lines 1, and 3-9) (Figure 1). In the north part of study area, one line from the TN152 cruise was extended from Golden Dragon seamount to Hole 801C and sited between the two lines from the TUNE08WT cruise (Lines 4-1,

3-9, and Line 92-1, -2) (Figure 1). For reference, we call these four survey subsets survey M34, survey H801, survey SOUTH, and survey NORTH.

2. Magnetic Data Processing

A total of about 1200 km of new track line data from the recent TN152 cruise were corrected and processed through the following steps: (1) gridding and filtering, (2) international geomagnetic reference field (IGRF) correction, (3) external field variation removal (e.g. Onwumechilli, 1967), (4) projection to a common azimuth, and (5) upward continuation to several levels.

In the first step, data points were gridded into 100 m separation using a spline routine. This step was required because of necessity of evenly spaced data in subsequent operations.

Both International Geomagnetic Reference Field (IGRF) and external field variation corrections were needed for the Mesozoic magnetic anomaly because the anomaly amplitudes are low. As for the IGRF correction, we removed the regional magnetic field by subtracting values obtained from the IGRF 2000 [Olsen *et al.*, 2000].

During the survey period of the TN152 cruise, external magnetic field variations were recorded by a base station magnetometer at Wake Island (19.17° N, 166.36° E) (Figure 1). To fill gaps in the Wake Island data, we used data from permanent observatories in Guam.

For external field variation corrections, we used data from Wake Island for most survey days, where such data were continuous and of good quality. For several days, for

which data from Wake Island were absent or unsuitable, we used data from the magnetic observatory at Guam. These data were filtered to obtain the long-wavelength diurnal external field variation, diminished to the daily average, and substituted for the missing parts of the Wake Island data. Calculated daily variations range from about 30 to 80 nT and average 50.4 nT. Corrected variation data were shifted in time by the difference in solar time between the station at Wake Island or Guam and the ship location, and were subtracted from the total field magnetic measurements.

Differences in ship track directions were addressed by projecting the processed total field magnetic measurements to a common azimuth of 135° to align them approximately perpendicular to previous mapped magnetic lineations.

The deep-tow magnetic profiles show such high resolution of small anomalies that it is often difficult to see the “big picture” and allow correlation with nearby tracks and sea surface data. To emphasize the longer wavelengths, deep-tow data were upward continued to three levels: 5.5, 3.0 and 0.0 (sea surface) levels. At 5.5 km level, removal of the depth variations of the magnetometer, which follows an uneven seafloor, was expected. Middle water (3.0 km) and sea surface levels were calculated in order to enhance longer wavelengths making correlations between magnetic profiles easier [Schouten and McCanny, 1972].

3. Correlation Models

Correlation models were made matching peaks and troughs of the magnetic anomaly series within each subdivision by eye. The purpose was to create the basis of a

reversal model using the redundancy of magnetic profiles. In the M34, H801C, and SOUTH surveys, correlations were made using the data at 5.5 km depth (Figures 2, 3, and 4), whereas correlations in the NORTH survey were made using new (L4-1) and old (L92-1 and L92-2) lines both at the mid-water and sea surface level upward-continued profiles (Figure 5). This allows us to more easily match larger anomalies, which can be used to help to correlate smaller anomalies.

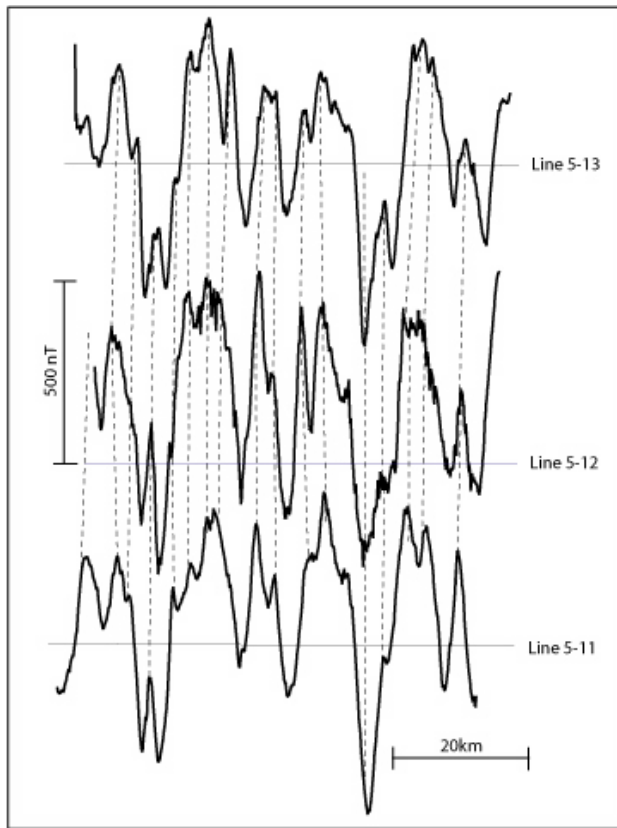


Figure 2. Correlation of magnetic anomalies among lines 5-11, 5-12, and 5-13 in M34 survey area. Dotted lines are correlations. Gray horizontal lines indicate zero crossing.

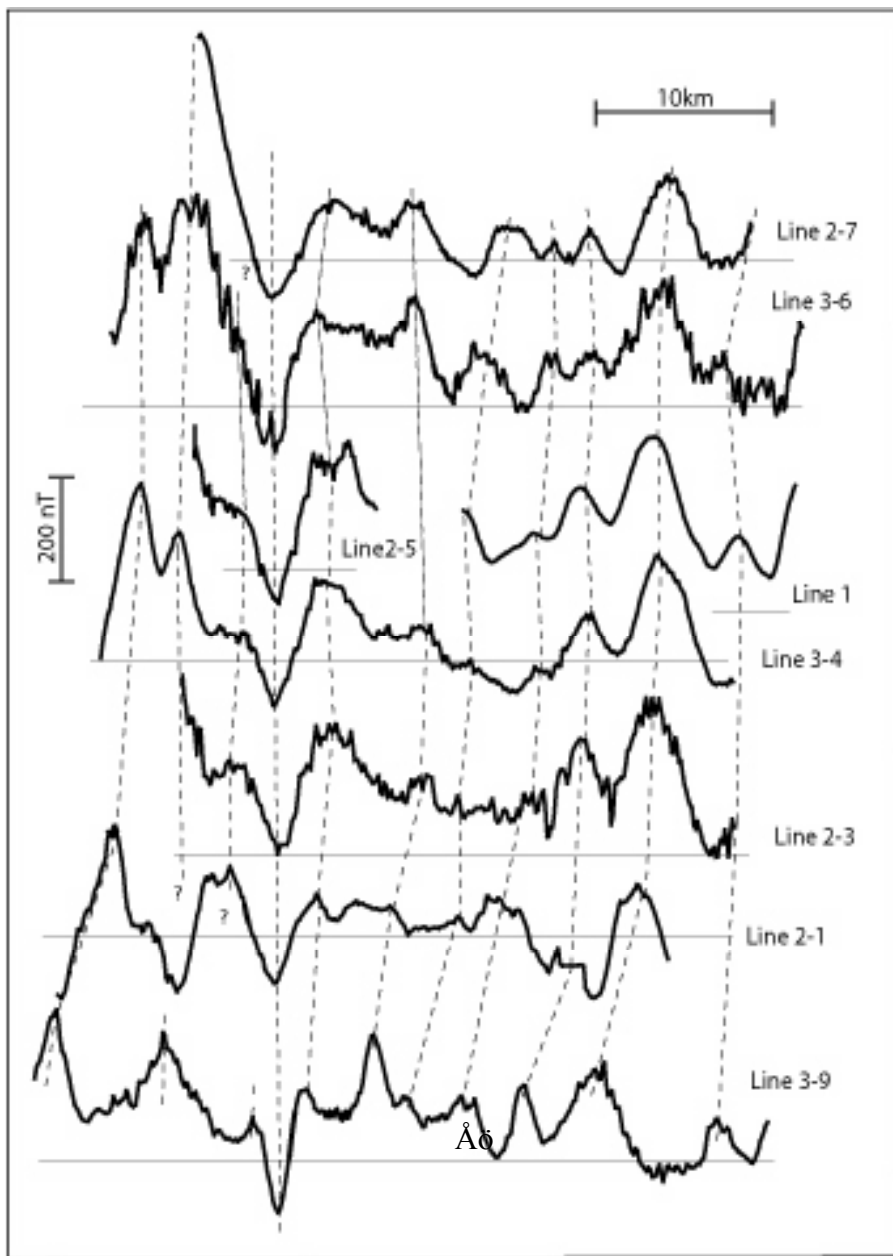


Figure 3. Correlation of magnetic anomalies among lines 3-9, 2-1, 2-3, 3-4, 1, 2-5, and 2-7 in H801C survey area. Dotted lines are correlations. Gray lines indicate zero crossing. Star shows approximate location of Hole 801C.

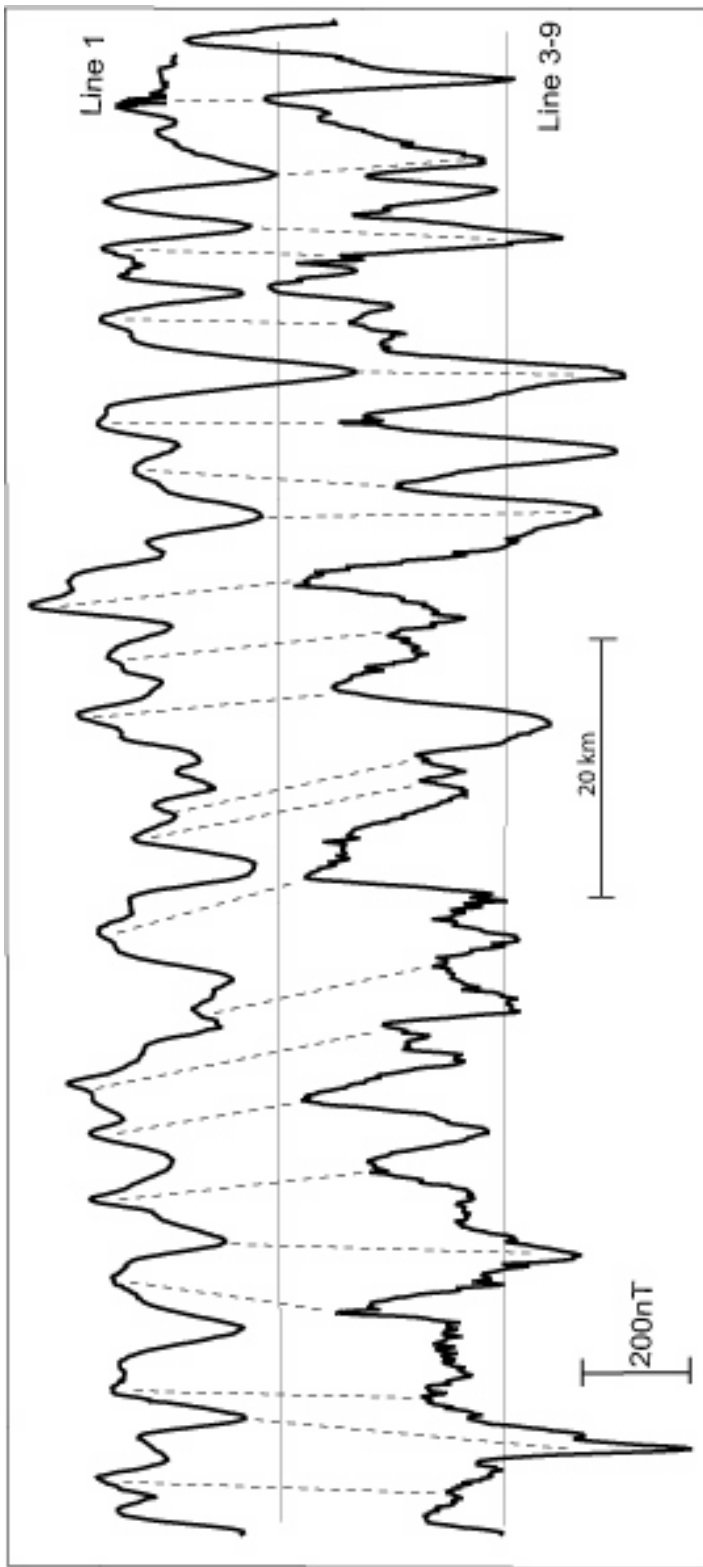


Figure 4. Correlation of magnetic anomalies between lines 1 and 3-9 in the SOUTH survey area. Dotted lines are correlations. Gray lines indicate zero-crossing.

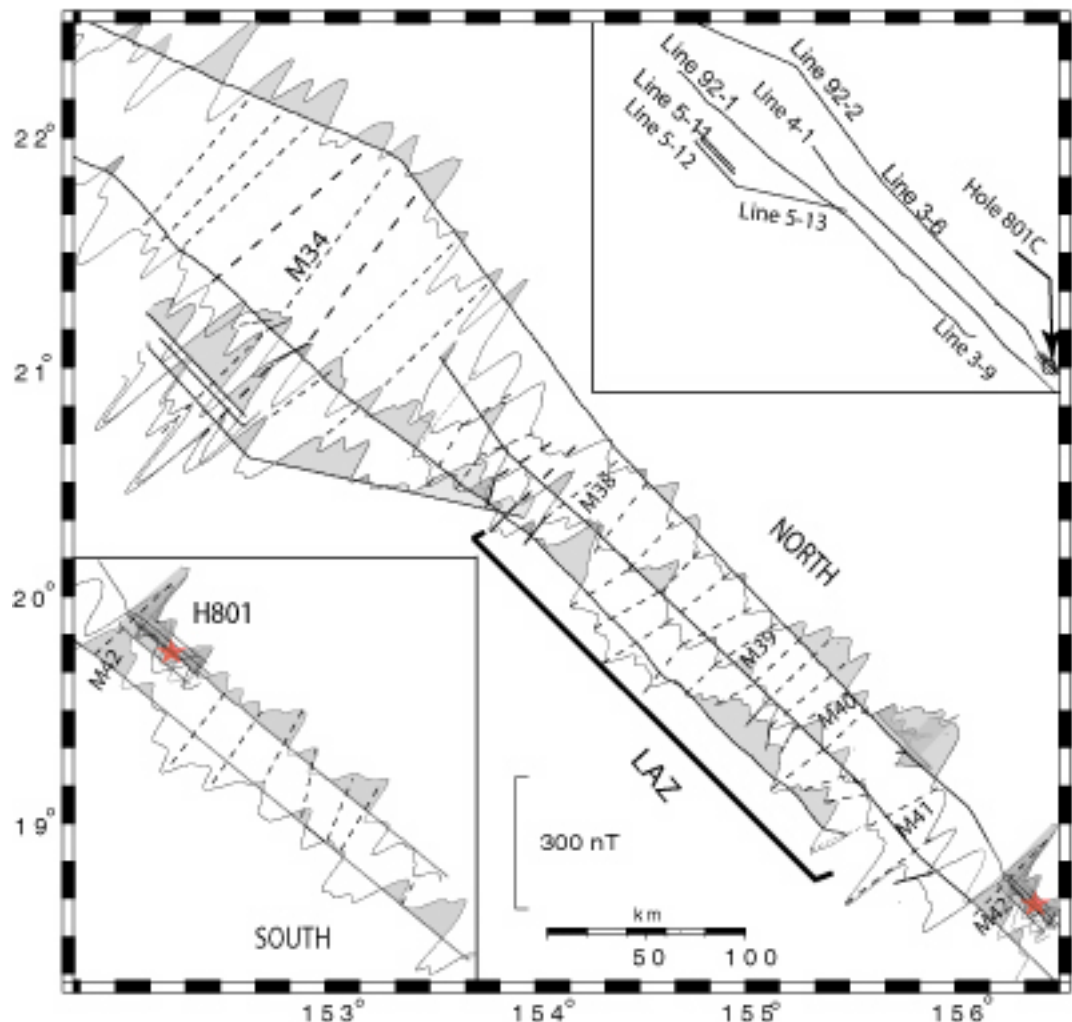


Figure 5. Correlation of magnetic anomalies from Sager *et al.* (1998) and this study in the NORTH survey area. Dotted lines are correlations among lines. NORTH= NORTH survey area (see text). LAZ= the low amplitude zone suggested by Tivey *et al.* (2005). SOUTH= SOUTH survey area (see text). Inset shows track lines and identifiers.

4. Magnetic Polarity Block Model

Our approach to making a polarity time series for the Jurassic deep-tow profiles was to use a potential field inverse modeling [Parker and Huestis, 1974] to make a preliminary interpretation of polarity and forward modeling [Parker, 1972] to finalize the interpretation. The inverse method was used to give an unbiased first estimation of polarity block boundaries. The forward model was then used to refine the model of the reversals.

For the modeling procedure, it was necessary to define appropriate values for the seafloor depth, sediment thickness, and thickness of the magnetic source layer. The seafloor depth and igneous basement were interpreted from the seismic profiles of Abrams *et al.* (1993). For simplicity, we used a constant depth of seafloor and basement for each survey site: 5.6 and 6.1 km for the M34 survey, 5.6 and 6.2 km for the NORTH survey, 5.5 and 5.9 km for the H801C survey, and 5.6 and 6.138 km for the SOUTH survey. Although there is no constraint for a thickness of magnetic source layer, typical GPTS models use it within the range of 500 – 1000 m. Therefore, a constant thickness of 1000 m was used for our modeling. For deskewing, we chose an ambient field inclination and declination calculated from the latitude and longitude of Hole 801C assuming a paleoinclination and declination of -0.2° and 20° respectively [Larson and Sager, 1992, Sager *et al.*, 1998]. Although the Pacific Jurassic paleolatitude and paleodeclination values are uncertain by 10 to 15°, the deskewing process is not sensitive to differences of this magnitude.

To determine a location of polarity block boundaries, we first assumed constant thickness layer with vertical polarity boundaries. Then, a Gaussian transition was applied to adjust the model and observed anomalies to obtain better fit between anomaly slopes [Schouten and Denham, 1979; Denham and Schouten, 1979]. Cande and Kent (1992a) suggested that magnetic modeling is not necessary because zero-crossings of deskewed anomalies can be used to determine polarity boundaries. However, because the Jurassic magnetic anomalies are low amplitude and have less distinctive short wavelength features, it is difficult to determine the polarity boundaries only by zero-crossings. Furthermore, the zero crossing is sensitive to a removal of long wavelength magnetic variation and an adjustment of the annihilator. Thus, we used zero-crossings only for first approximations.

Inverse modeling requires removal of short and long wavelengths to obtain realistic magnetization models; so wavelengths less than 2.0 km and more than 140 km were filtered out. Both wavelengths were chosen to avoid making unnecessary changes in original anomaly features.

We next created polarity block models based on anomaly correlation and inverse modeling, then used them as a magnetization distribution model for the forward modeling. When we established magnetic polarity models, magnetization strength was assumed from the standard deviation of the magnetization values calculated by inverse modeling. We aimed to produce a satisfactory match of observed and calculated anomalies. Although Sager *et al.* (1998) applied exponential reduction in the magnetization strength with the initial magnetization as 2.25 Am^{-1} , we did not find it a

good approximation in this study because anomaly amplitudes are adequately modeled with a constant magnetization in the several study areas. Constant magnetization values were used in each survey areas based on our satisfactory matchings between observed and calculated anomalies: 2.0 A/m for the NORTH survey, 1.68 A/m for the H801C survey, and 2.3 A/m for the SOUTH survey.

5. Composite Model

We combined magnetic polarity block models from subparallel lines to make composite polarity boundary models. The purpose in this process was to create a composite model of reversals that appear common to all lines within a given survey area. From the Sager *et al.* (1998) study, we adopted the composite model for the two previous deep-tow lines (Line 92-1 and -2). The boundaries of each polarity block in the composite model was calculated by averaging values of corresponding block boundary distances among the polarity model series. In the case that we had two blocks on one line and one block on the other, the two blocks were merged as one reversal in calculate the composite model.

6. Age Calibration Model

In general, the Mesozoic magnetic polarity series has few good absolute age calibration points to interpolate or extrapolate the ages of chron boundaries. Sager *et al.* (1998) used the radiometric date of M26r (155.3 Ma) from the Argo Abyssal plain [Ludden, 1992] because it was possible to tie 1992 deep-tow lines to that anomaly in the

Pigafetta Basin. They extrapolated age of blocks from M25 onward using existing GPTS [e.g. Gradstein *et al.*, 1995; Handschumacher *et al.*, 1988]. Our approach in this study was to use absolute ages for M26r and Hole 801C as a tie points on both ends of the survey lines, with linear interpolation in between assuming a constant spreading rate. In our survey, Hole 801C lies on the track line (Figure 1), and a new high-precision age determination for the tholliitic basalt layer (167.4 Ma) by Koppers *et al.* (2003a) is used for the age at that location.

RESULTS

1. Correlation Model

The correlation of anomalies in our study ranges from excellent to fair. The best was the M34 survey where anomalies closely matched on adjacent lines. In contrast, the worst was the NORTH survey, which contains small, difficult-to-correlate anomalies.

In the M34 survey, where the anomaly amplitude was relatively large (~ 500 nT), the correlation was easy because the anomalies show only small differences (Figure 2). Another region of easy-to-correlate anomalies was around the H801C survey, where anomaly amplitudes are mostly < 200 nT (Figure 3). In this area we were aided by having many closely spaced lines for correlation. The anomalies in this survey display similar amplitudes, widths, and shapes, and even small features are usually similar from one line to the next. Anomalies in the SOUTH survey have relatively large amplitudes, (~ 200 nT). Although we have only two lines, they display general agreement of large anomaly shapes and locations, albeit with considerable variation in smaller features (Figure 4). Therefore, that most anomalies are correlatable, consistent with seafloor spreading magnetic lineations.

The NORTH survey was the most difficult region to correlate because it contains anomalies both large and small, which are hard to match uniquely among the few available lines (e.g. Figure 5). North of $\sim 21^\circ$, the anomalies are large, but difficult to match between lines. South of 21° , inconsistency in the shapes and spacing of larger anomalies makes it difficult to correlate either the large and small anomalies (Figure 4,

5). This area of difficult correlation corresponds to M35 – M38 from Sager *et al.* (1998).

The zone of smallest anomalies, from 21° to 18.5°, was termed the low amplitude zone (LAZ) by Tivey *et al.* (2005).

In our model, the new deep-tow line is not correlated well to the old lines because the shape and amplitude of anomalies on the new line are often different from those on the old lines. This result shows that the single new line did not significantly improve the correlation. Nevertheless, the positions of small anomalies relative to the longer-wavelength features on the upward continuation profiles (middle and sea surface levels) made it possible to make nearly one-to-one correlation between old and new anomalies (Figure 5). In old-new lines correlation, we made several observations. First, correlation from M34 northward is good, with similar anomaly shapes, even though this correlation is based mainly on 2 lines from Sager *et al.* (1998). Then, correlation from M34 to M42 is problematic because (a) large anomalies do not often match well, particularly in M39 – M41 where we have even close lines and (b) regular pattern of small anomaly features suggest correlations of nearly one-to-one match and similar to Sager *et al.* (1998). Lastly, anomalies between M38-M41 have distinctly smaller amplitudes than those to north and south part of M38- M41 (i.e. LAZ, Tivey *et al.*, 2005) (Figure 6).

2. Magnetic and Composite Model

Because the magnetometer was closer to the seafloor, this study provides for a higher resolution polarity block model compared to Sager *et al.* (1998). The polarity

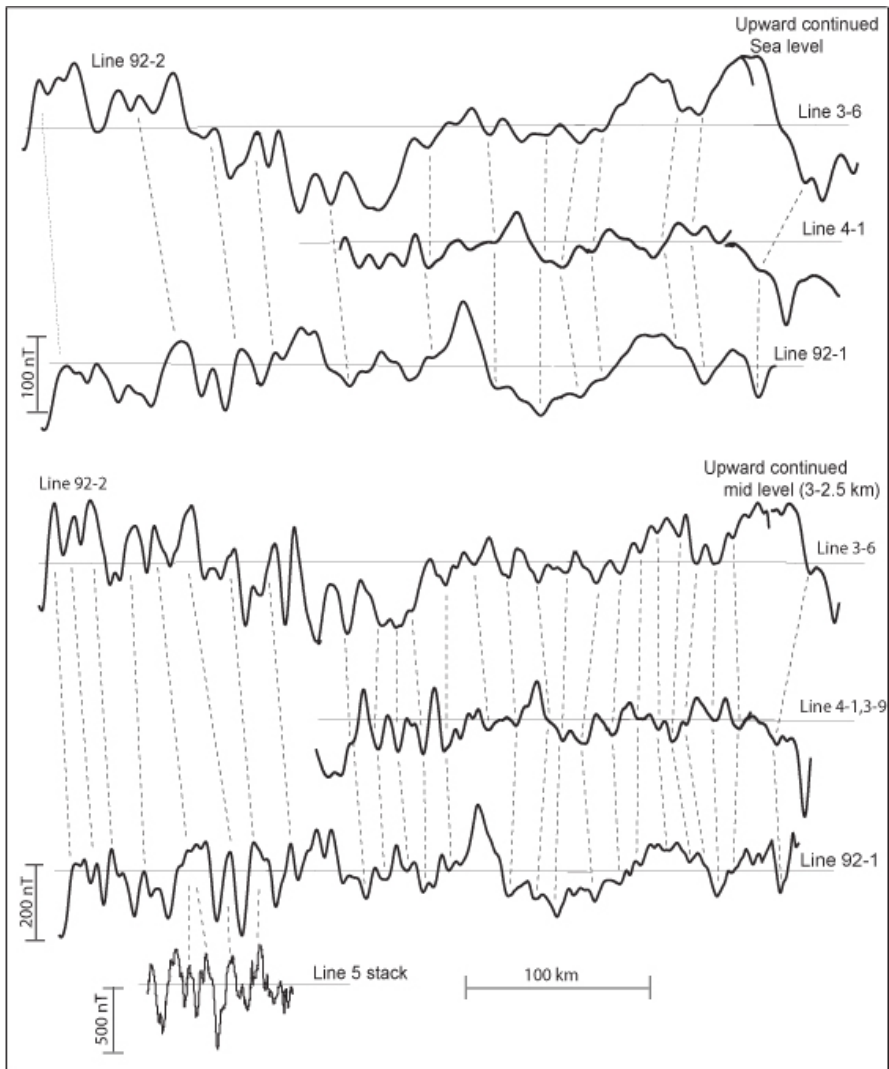


Figure 6. Correlation of magnetic anomalies among lines 5, 92-1, 4-1, 3-9, 3-6, and 92-2 in NORTH survey area. Lines 5-11, 5-12, and 5-13, over M34, were stacked as line 5 in this figure. For mid-water upward continued model, line 92-1 and 92-2 have 2.5 km depth, and Line 5, 4-1, 3-9, and 3-6 have 3.0 km depth. Dotted lines are correlation among the lines. Gray solid lines indicate zero crossings. Note that vertical scale for mid-water and sea surface level is different.

blocks around the area of M34 are consistent with those modeled by Sager *et al.* (1998) (Figure 6). This makes it easy to composite the polarity model.

Both H801C and SOUTH models have many small, coherent anomalies, and short duration of modeled reversals because our polarity reversal model was matched to detailed features on the observed anomalies. For example, the composite model of H801C, which was stacked from correlated lines (Figure 7), shows total of 16 reversals in 20 km. In the SOUTH survey, the composite model from two correlated lines has total 34 reversals in 120 km (Figure 8). We also constructed a composite model using upward continued profiles (3.0 and 0.0 km) for both the areas of H801C and SOUTH. The composite model of Sager *et al.* (1998) was compared to these models (Figure 9). In our composite model, the areas of H801C and SOUTH show good similarity with similar number and width of blocks, even though we see some small differences.

In the composite model of new and old lines in the NORTH survey, most of the high frequency, short duration reversals on the new profile (e.g. 40 reversals in 100 km) were not retained in the composite model based on spectrum analysis explained below (Figure 6). This makes the composite model of NORTH similar to that of Sager *et al.* (1998).

After the making of composite polarity block model, additional adjustments were made to finalize our model. To determine whether noise from the process of crustal magnetization, the external field, or elsewhere (e.g. artifacts during the survey) caused the short-wavelength anomalies we used a spectral amplitude analysis that is generally applied to calculate the depth of the magnetic source layer [Spector and Grant, 1970;

Nwogbo, 1998]. Deep-tow Line 4-1 and 3-9 were used to calculate spectra because these lines cover NORTH, H801C, and SOUTH regions. We first subdivided the lines into two sections, part A and B, expecting the changes in the spectra because of the different appearance of wavelengths (Figure 10). Lognormal plots of spectral amplitude show two approximately linear sections with a break in slope at 0.9 km^{-1} in Part A and 0.7 km^{-1} in Part B. The shape and approximate break points are nearly consistent with that of Sager *et al.* (1998) and indicate the transition between signal and noise. The almost flat short-wavelength section is usually interpreted as a noise component [e.g. Parker, 1997]. In detail, curve B is above curve A at short wavelength which implies higher power at shorter wavelengths. As the average break point between on the spectra of Part A and B was 1.2 km (0.8 km^{-1}), we can consider it is inappropriate to retain polarity blocks less than this length.

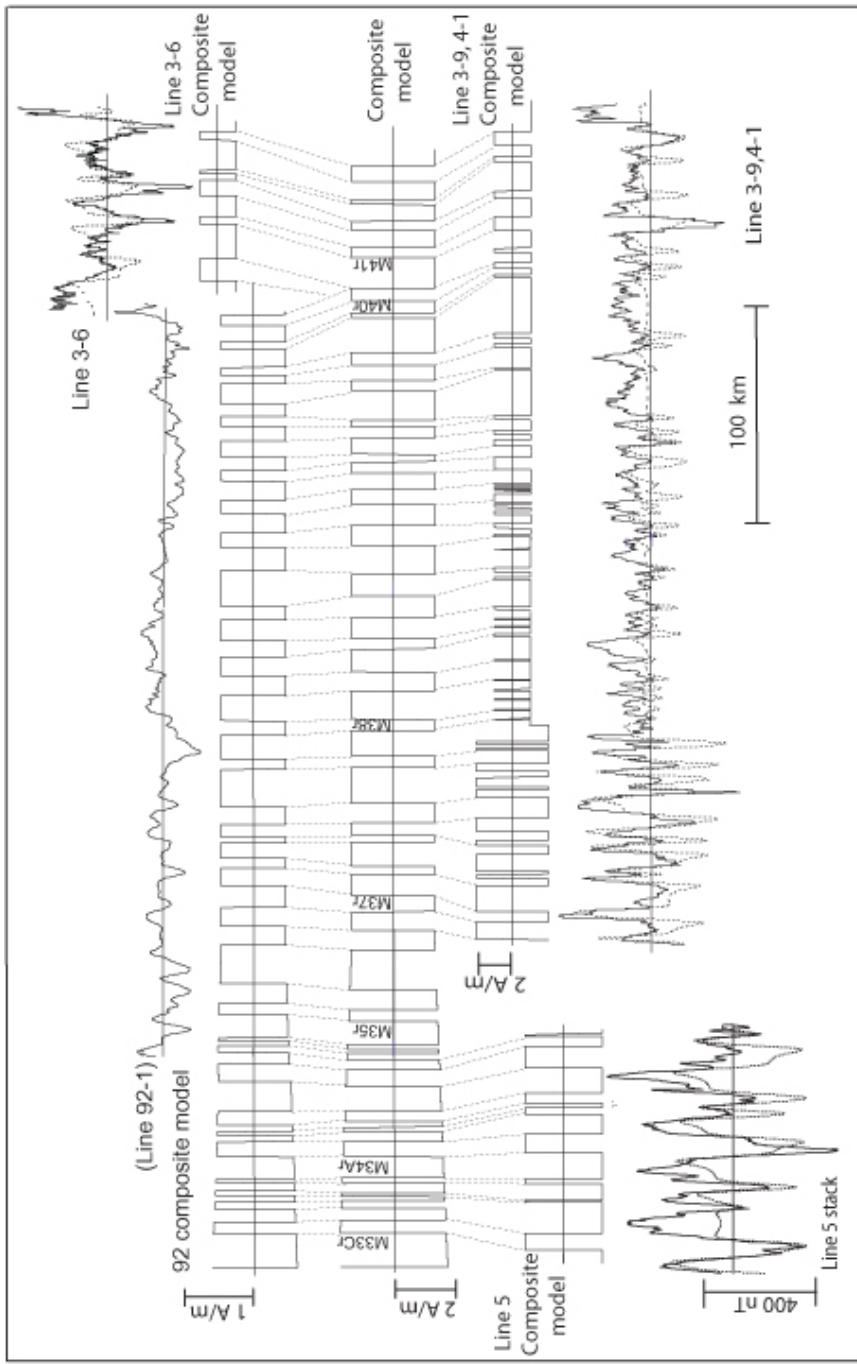


Figure 7. Composite model of magnetic polarity block model established in study of Sager *et al.* (1998, 92-composite model) and this study. Solid magnetic anomalies are observed anomalies. Dotted magnetic anomalies are calculated anomalies (see text). Horizontal lines indicate zero crossings. Note that each vertical scale is different. Line 92-1 appears opposite in polarity from new lines because the anomaly profiles shown in Sager *et al.* (1998) were deskewed.

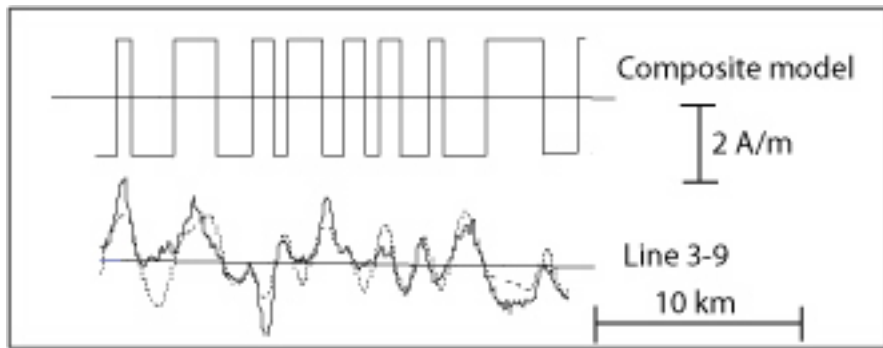


Figure 8. Composite magnetic polarity block model of the deep-tow profiles around Hole 801C. Line 3-9 in this figure is shown as a reference of anomaly profiles of lines 3-9, 2-1, 2-3, 3-4, 1, 2-5, 3-6, and 2-7.

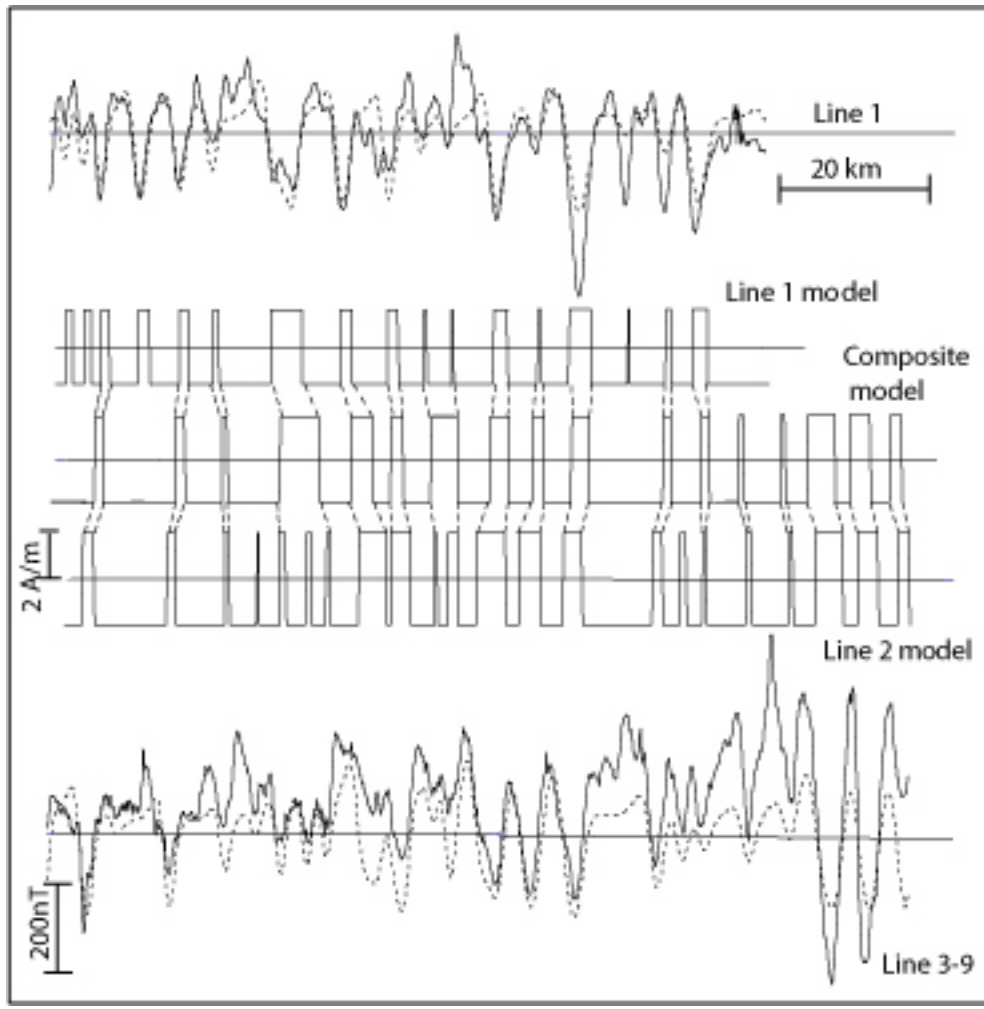


Figure 9. Composite magnetic polarity block model of the deep-tow magnetic profiles of the SOUTH survey area. Solid magnetic anomalies are observed anomalies. Dotted magnetic anomalies are calculated anomalies. Horizontal lines indicate zero crossings.

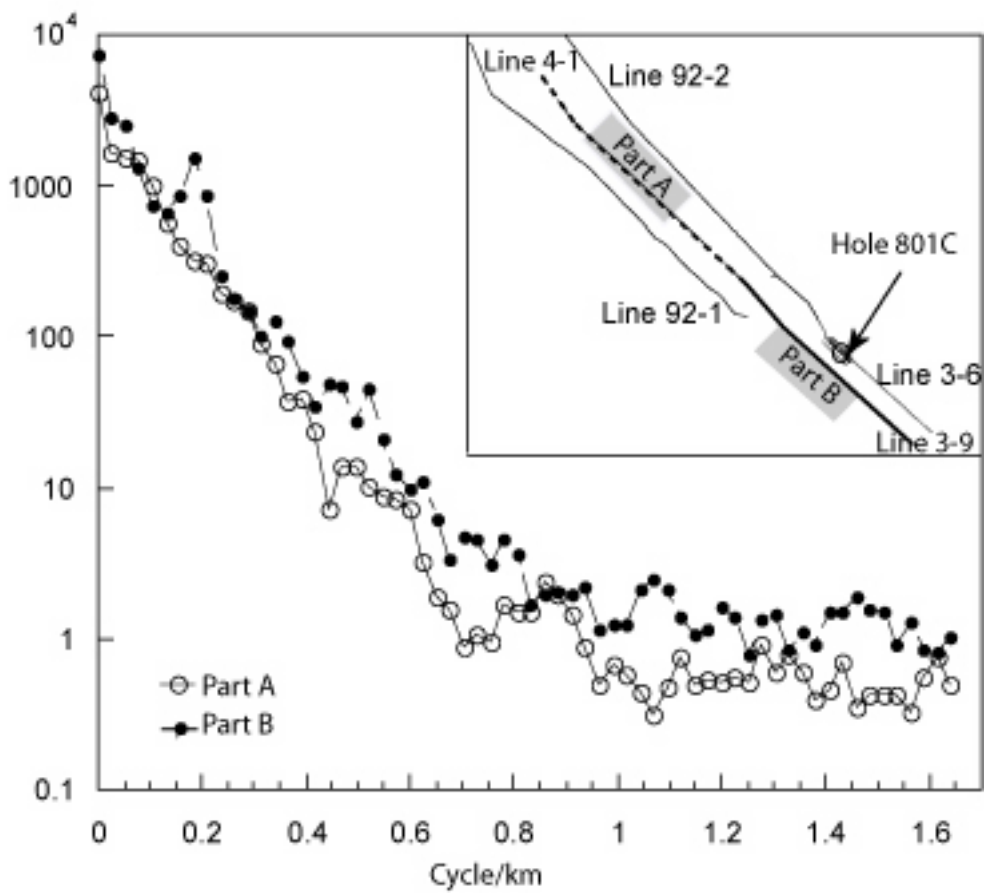


Figure 10. Power spectra of two segments of line 4-1. Note that vertical scale is logarithmic.

3. Age Calibration

The age of each polarity boundary was determined with linear interpolation and extrapolation using the age-distance equation of $\text{Age} = 0.0146 \times \text{distance} + 155.3$ m.y. (Figure 11).

Subsequently, we calculated the distance between M26r [Ludden, 1992] and youngest chron (M27) in Sager *et al.* (1998) to interpolate the age of M27 and others. The Age-distance curve suggests some uncertainty in the GPTS age model because of the uncertainty of the radiometric ages (Figure 11). The maximum and minimum half spreading rates are, 117.2 km/m.y. and 48.1 km/m.y., respectively taking the maximum and minimum slopes of lines that stay within the error bars of the dates. We used the upward continued, sea surface level model to determine chron numbers to be comparable with previous GPTS studies that used sea surface level data (Figure 12) [e.g. Handschumacher *et al.*, 1988; Cande and Kent, 1992a; Sager *et al.*, 1998]. Our new GPTS models from deep-tow and middle level continuation modeling are shown in Figure 13. For a comparison, we also show the models from Sager *et al.* (1998) and Handschumacher *et al.* (1988). With our age calibration, the GPTS is extended to M 44 at 169.4 Ma.

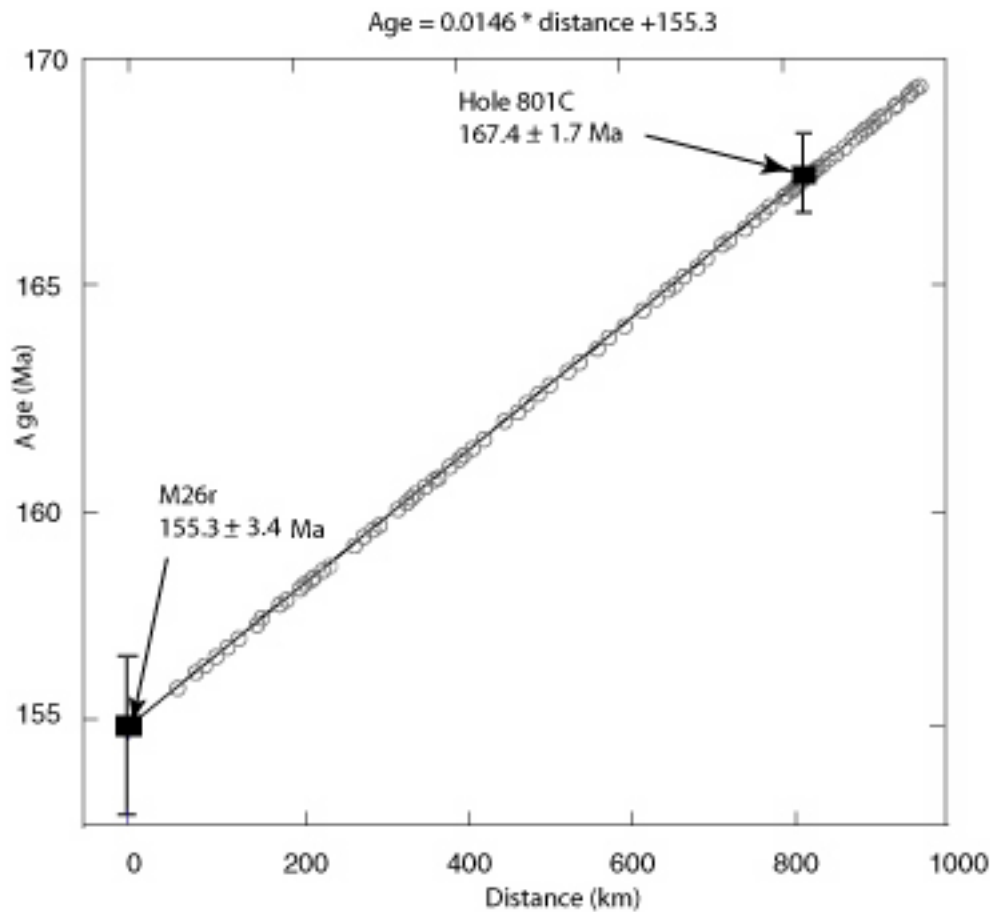


Figure 11. Age calibration using two absolute ages from ODP sites. Open circles indicate deep-tow magnetic polarity boundaries. Square indicate the absolute ages corresponding to the polarity boundaries on the magnetic composite model. Error bars show 1 sigma of radiometric age datings. Equation on the top of this figure is age-distance relationship from linear interpolation between two anomalies.

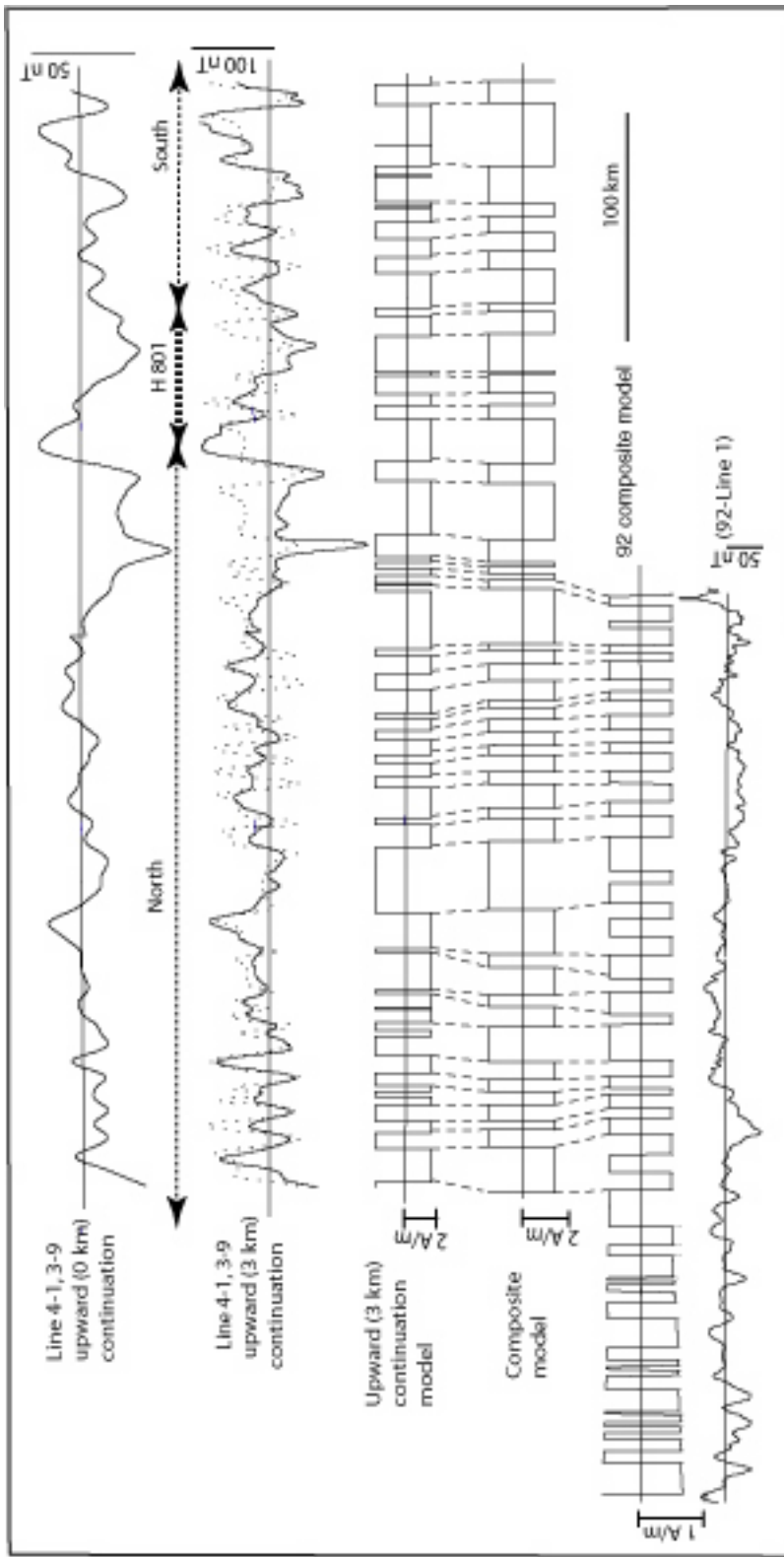


Figure 12. Composite magnetic polarity block model at mid-water level, upward continued magnetic profiles. As a comparison, sea level upward continued anomalies are also shown. Solid magnetic anomalies are observed anomalies. Dotted anomalies are calculated anomalies. Note that the vertical scale for each magnetic profile is different.

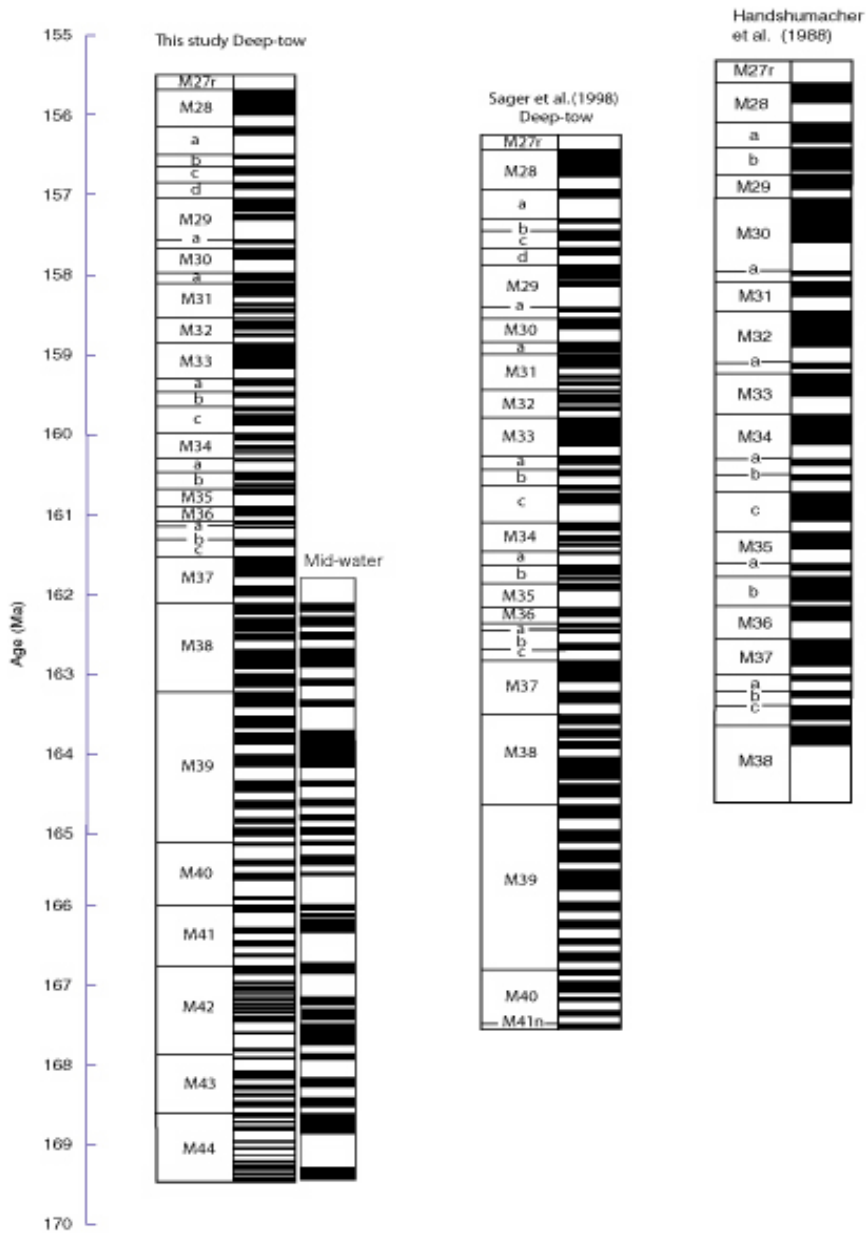


Figure 13. Deep-tow and mid-water magnetic polarity model from this study compared with that of *Handshumacher et al.* [1988] and *Sager et al.* [1998]. Black stripes show normal and white stripes show reversal polarities. The age of each polarity block boundary is given in Table 1 and 2 (Appendix A).

DISCUSSION

In this study we have correlated magnetic anomalies in the Pacific JQZ using approximately 1200 km of new deep-tow magnetic profiles that complement 1480 km of deep-tow data collected by Sager *et al.* (1998). The new data augment the previous study in several ways. Closely-spaced lines examine detailed correlation of small anomalies in two small areas around M34 and Hole 801C. These new data also provide additional lines in the area of uncertain anomaly correlations from the previous study, as well as lines that connect Hole 801C with the previous study and extend it southeast to the rough-smooth boundary of Handschumacher *et al.* (1988). Furthermore, the additional data allow us to address several questions: (1) are the smallest anomalies mapped in previous JQZ studies correlatable?, (2) are correlatable anomalies found deeper in the JQZ?, (3) are apparent reversals in the 474 m basalt section cored at Hole 801C representative of surrounding magnetic lineations?, and (4) what are the implications for the cause of JQZ?.

1. Correlation

The deep-tow profiles collected as closely-spaced lines around anomaly M34 show excellent correlation of both small and large anomalies. Correlation of anomalies around Hole 801C is also quite good. Although not as robust as that of the M34 and Hole 801C sites, correlation on the two lines south of Hole 801C is good for large anomalies, as is the correlation of anomalies in the northernmost area surveyed, from

M34 northwestward. In sum, most surveyed anomalies appear strongly linear and similar to other seafloor spreading anomalies in different locations around the world.

In contrast, anomaly correlations are difficult in a 300 km long zone in the south part of the NORTH survey area. This section has the smallest anomalies measured, so we call it the LAZ [Tivey *et al.*, 2005]. It corresponds to M38 through M41 of Sager *et al.* (1998), the part of their study with smallest anomalies and poorest correlation. Although the closely spaced tracks around Hole 801C show that even small anomalies are correlatable in the area, similar anomalies in the LAZ are difficult to match from line to line with certainty. The difference in anomaly correlatability suggests either anomalous behavior of the paleomagnetic field or changes in tectonic setting (e.g. seafloor spreading) in the area. That is to say, (1) the magnetic field may have had rapid reversals or fluctuations that were too frequent to make strongly linear anomalies or (2) the magnetic recording was degraded because of ridge jumps, propagating rifts, or similar mechanisms.

2. Reversal Models

In making reversal models of the deep tow magnetic lines, we have made the traditional assumption that anomalies result from magnetic reversals recorded by seafloor spreading [Vine and Matthews, 1963]. Although this assumption has been highly successful in creating GPTS models, several studies suggest that small anomalies may not always represent polarity reversals.

The main alternative to reversals is fluctuations of paleofield intensity, which have been observed in high-resolution magnetic profiles [e.g. Cande and Kent, 1992b; Bowers *et al.*, 2001]. Statistically, reversals and paleointensity fluctuations likely result from the same set of geomagnetic instabilities, implying that they appear similar in magnetic profile data [Marzocchi, 1997]. In magnetic reversal modeling, interpreting small anomalies is troublesome because the nonuniqueness of potential field modeling makes it difficult to determine which small anomalies represent real polarity reversals and which are simply intensity fluctuations. For their widely accepted GPTS model, Cande and Kent (1992a, 1992b) arbitrarily rejected chrons with durations shorter than 30 kyr, arguing that smaller anomalies likely result from paleointensity fluctuations. Similarly, Sager *et al.* (1998) constructed a Jurassic GPTS with a reversal for every magnetic anomaly, but preferred a model filtered by upward continuation to mid-water depth because it contained reversals only for the larger anomalies.

To distinguish between reversals and intensity fluctuations, several investigator groups have compared sedimentary magnetostratigraphy with small anomalies in magnetic profiles. Lenci and Lowrie (1997) suggested that “cryptochrons” within C12 and C13 in the timescale of Cande and Kent (1995) are paleointensity fluctuations rather than magnetic reversals because of a lack of corresponding polarity reversals in contemporaneous sediment cores.

On the other hand, even if the sedimentation rate seems to be enough to preserve the magnetic reversals, whether the cryptochrons appear in any sedimentary record or not is another issue. In contrast to Roberts and Lewin-Harris (2000), who concluded

small anomalies in C5 are attributed to polarity reversals, Bowers *et al.* (2001) and Bowles *et al.* (2003) argued the anomalies are paleointensity fluctuations based on strong correlations between deep-tow magnetic profiles and sedimentary relative paleointensity records [Bowers *et al.*, 2001; Bowles *et al.*, 2003].

However, such conclusions are weakened by observations that sediments may not record all short reversals. The resolution of sedimentary paleomagnetic records depends significantly on sedimentation rate; thus, small anomalies may be averaged out if the sedimentation rate is low [Roberts and Winklhofer, 2004]. The fidelity of sedimentary records may only be satisfied when the records show spatial consistency in several sites around the world. For example, Acton *et al.* (2005) reported several ODP sites around world's ocean where the cryptochrons were identified in the sedimentary records.

With this fundamental uncertainty in mind, we made two Jurassic GPTS, following the methods of Sager *et al.* (1998). Our GPTS models extend further back in time to 169 Ma, approximately 2 million years older than the GPTS by Sager *et al.* (1998). For one model, we assumed that every small anomaly results from a polarity reversal. This gives the maximum number of possible reversals. An alternative GPTS was constructed from the deep-tow magnetic profiles upward continued to mid-water depth. This model likely gives an underestimate of the number of polarity reversals. Because it is approximately 3 km above the source layer, the mid-water GPTS model is comparable to other GPTS constructed from magnetic profiles over younger oceanic lithosphere. We did not apply a 30 kyr cut-off, as did Cande and Kent (1992a), because it appears an arbitrary value.

Both deep-tow and mid-water GPTS models include polarity durations shorter than 30 kyr; 12.5 % and 3 % of the total number of polarity blocks, respectively. The deep-tow model of the LAZ and H801C survey areas shows many short polarity reversals between 14 - 233 kyr (average 99 kyr) duration. In these areas, approximately 15% of the modeled reversals have less than 30 kyr durations. Interestingly, in places the modeled polarity bias seems to shift between deep-tow and mid-water model, particularly around Hole 801C. While the deep-tow model of this area seems to show mostly normal polarity, the upward continued model seems predominantly reverse polarity (Figure 13). This difference occurs because of the upward continuation, which blends low amplitude deep-tow anomalies into larger, middle depth anomalies that sometimes appear opposite from the deeper signal.

3. Correlation between Our Models and Hole 801C Data

Although there are fundamental ambiguities about the interpretations of reversals on our GPTS models, two sets of data, downhole logging data from Hole 801C and the Jurassic magnetic stratigraphy from continental sedimentary sections, support the existence of short polarity periods, implying a rapid reversal frequency.

Both paleomagnetic and downhole logging data are available from the 474 m basalt section cored at Hole 801C. Both data sets imply six reversals in the section [Wallik and Steiner, 1992; Steiner, 2001; Tivey *et al.*, 2005]. Under the classic assumption of vertical polarity boundaries in the oceanic crust, there should be no reversals in this section. In contrast, if tilted magnetization boundaries are assumed

within the oceanic crust, changes in magnetic polarity can occur within a vertical hole. Thus, magnetic reversals appearing as surface magnetic anomalies around the hole may well be actual polarity reversals based on this assumption.

With the data from Hole 801C, the reversal rate is uncertain because of poor constraint on the duration of volcanism; however, the authors have given estimates of 60 to 100 rev/My based on assumptions of the duration of crustal construction [Steiner, 2001; Tivey *et al.*, 2005].

In M42 on our GPTS models, corresponding to H801C survey area, the deep-tow model shows the reversal rate of 12 rev/My (1 rev/ 83 kyr). The mid-water model, which leaves out the smallest anomalies, gives only 4 rev/My (Figure 13). Both reversal rates are less than the bounds implied by the logging and paleomagnetic data from Hole 801C. Compared with the present-day (C1n) reversal rate, 12 rev/My of deep-tow model is factor 9 [e.g. Cande and Kent, 1992a]. However, the highest Neogene reversal rates occur in polarity subchron (C2r.1n) and cryptochron (C10r-2) on the Cande and Kent's GPTS model (1995) show 1 rev/100 kyr and 1 rev/ 70 kyr respectively suggesting high reversal rate of the 12 rev/My is not extreme.

High reversal rates in the Jurassic have been also interpreted from continental magnetostratigraphic studies [Steiner *et al.* 1987; Steiner, 2001; Ogg and Smith, personal communication, 2004]. The Jurassic continental magnetostratigraphy has been pieced together from various locations in Europe [Ogg and Smith, personal communication, 2004]. Although there still remains a lack of continuity in the magnetostratigraphy, many short reversals in upper Bajocian (~ 8 rev/My), Bathonian (~

8 rev/My), and Callovian (\sim 6 rev/My) indicate fair consistency to our GPTS models [Steiner *et al.*, 1987; Ogg and Smith, personal communication, 2004].

The estimation of reversal rates from Hole 801C seems to be extremely as high, greater by a factor of 5 compared with our GPTS models. From Figure 12, 60 rev/Myr (1 rev/ 17 kyr) can be calculated as 1.14 km for one polarity block whereas our estimation of 12 rev/Myr has 5.7 km for one block. These numbers make us wonder if reversal rates from Hole 801C have not been over estimated because of incorrect assumptions about the construction rate of the crust (e.g. Tivey *et al.* 2005). Points that should be considered are: (1) the 1.14 km (1 rev/17 kyr) polarity block should be detectable from deep-tow anomaly profiles around Hole 801C area, and (2) considering geomagnetic field behavior, 17 kyr reversals hardly gives the field enough time to reverse (McFadden and Merrill, 1993). At a width of \sim 1 km, even if such polarity block is detected, it would be difficult to correlate or possibly ignored as a noise. Simultaneously, it should be noted that some of polarity reversals on our GPTS have similar short durations as the 17kyr (Table 1), so that the 5.7 km polarity block indicates only average of various polarity blocks. Similarly, the 17 kyr reversals (60 rev/Myr) indicate only a possible reversal rate based on an interpretation about accretion process in the oceanic crust around Hole 801C by Tivey *et al.* (2005). As long as a relationship between applied absolute ages and lithological boundaries in the basalt section of Hole 801C likely be changed, it is plausible to assume the reversal rates from Hole 801C may also be lower than the 17 kry reversal rate.

Although there is an apparent difference in reversal rate between our study and the Hole 801C interpretation, we conclude that the difference could be attributed to uncertainties in the interpretation of the latter results. Thus, it is plausible that lineated magnetic anomalies around Hole 801C are attributed to actual magnetic reversals.

4. Implications for the Origin of the JQZ

Systematic changes in anomaly amplitudes are observed along the deep-tow lines. Anomalies decrease toward the southeast (i.e. increasing in age) continuing the trend that has been noted by other authors [e.g. Cande *et al.*, 1978; Sager *et al.*, 1998], and reach minimum amplitude and shortest wavelength in the LAZ. Farther southeast, the anomaly amplitudes increase slightly south of Hole 801C. The systematic changes in the amplitude suggest changes in paleomagnetic field strength, perhaps related to reversal rate. The field intensity seems to have decreased until reaching a minimum during the LAZ, where the fluctuation rate was highest, and then increased through the late Jurassic as reversal rate declined.

Changes in anomaly amplitudes on the deep-tow profiles, particularly around the LAZ, may give clues about the origin of the JQZ. There are several hypotheses to explain the changes: (1) long-term changes both in the crustal magnetization and in Earth's magnetic dipole field, and (2) overlapping of intensity lows because of interference of rapid magnetic field reversals, (3) closely-spaced reversals in the oceanic crust, and (4) changes in Pacific Jurassic tectonics for the changes around the LAZ.

In terms of long-term changes, a decrease in anomaly amplitude backward in time has been explained with systematic changes in the oceanic crustal magnetization over last 160 million years [Johnson and Pariso, 1993]. However, it is not plausible to assume that the decrease from M34 through the LAZ is a result of degradation of crustal magnetization because this degradation occurs exponentially only in first several million years after crustal formation. Long-term change is suggested by the behavior of the Earth's magnetic field: the Jurassic was a period of magnetic dipole field intensity low [e.g. Prévot *et al.*, 1990; Heller *et al.* 2003; McElhinny and Larson, 2003; Thomas and Biggin, 2003; Biggin and Thomas, 2003]. We prefer to assume that the Jurassic dipole intensity low somewhat contribute to lessen the anomaly amplitudes over the JQZ.

Sudden change in the anomaly amplitudes from relatively large to low at northern edge of the LAZ requires additional rationalization because the geomagnetic field behavior is unusual. It seems that the anomaly amplitudes in the LAZ indicate a period of polarity transition that has been observed as a period of having approximately 25 % of full reversal intensity [e.g. Kristjansson, 1995; Merrill and McFadden, 1999]. However, the duration of the LAZ (4 m.y.) might be too long to be considered as a single polarity transition. One candidate to explain peculiar low anomaly amplitudes in the LAZ is overlapping of intensity lows because of interference of rapid magnetic field reversals. Valet *et al.* (2005) suggested that the more magnetic field becomes weak, the more reversals may occur. We presume that rapid reversal rates in the period of the LAZ were induced by the Jurassic dipole low so that the intensity was not fully recovered.

Together with the overlapping intensity lows, the magnetization structure observed in Hole 801C also contribute to low anomaly amplitudes in the LAZ. The vertical magnetization structure observed in Hole 801C may indicate that the magnetic polarity boundaries are tilted and the boundaries are closely spaced around Hole 801C. If this magnetization structure in the oceanic crust extended to the north of the H801 survey area, where the LAZ is located, it is appropriate to assume that the LAZ has similar polarity reversals within the tilted oceanic crust. If this hypothesis is true, presumably some diminution of anomalies may occur from field cancellation by closely spaced blocks of opposite polarity [Johnson and Merrill, 1978]. To test the plausibility of this assumption, we calculated simple forward modeling with arbitrary tilted polygon [Talwani and Heirtzler, 1964]. For simplicity, we assumed 1 km thickness for the source layer and made two different models with 0° and 53° tilt angles, examining various polarity widths (the 53° angle of the tilted magnetization boundary is consistent with the observed dip from Hole 801C (Pockalny and Larson, 2002)). Overall intensity of tilted source layer is less than non-tilted source layer (Figure 14). Interestingly, we see 40 % reduction of the intensity of both non-tilted and tilted structure when a polarity width is less than ~ 5 km (Figure 14). This narrow polarity width that induces low intensity is consistent with polarity width calculated from Hole 801C reversal rate (60 rev/Myr = $1.14\text{km}/$ polarity block). With these results, we suggest that tilted magnetic source layer in the JQZ may contribute to reduce overall intensity of magnetic anomalies when the reversal rate is high. In other words, the abrupt change could be caused from polarity block width crossing the threshold $\sim 5\text{km}$ as shown in Figure 14.

Tectonic complications to spreading in the Pacific JQZ are poorly known. If there are tectonic complications, such as ridge jumps or propagating ridges, we would expect disturbed, difficult-to-correlate anomalies. Because of the paucity of information, we barely can identify detailed tectonic setting around the LAZ. Addition to that we suggested above, if there is a complexity in the oceanic crust (i.e. ridge jumps), it easily results in unusual magnetic signatures. Perhaps, many, closely spaced survey tracks in the LAZ like H801C survey area may resolve this issue because poor correlatability of the magnetic profiles seem to partly disturb further investigations about the LAZ. Although it is also hard to say the correlatability among the magnetic profiles depends on density of the profiles comparing to H801C survey area, we suggest that the origin of the LAZ may not be identify without further investigations in the tectonic settings.

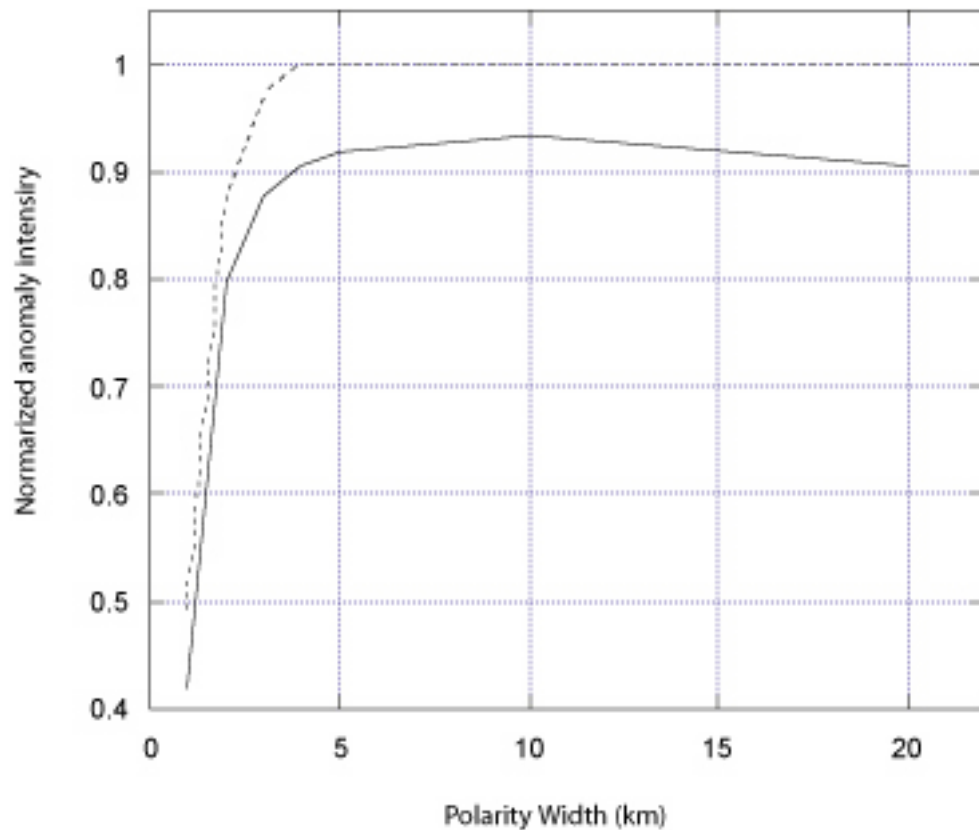


Figure 14. Calculated anomaly intensities with various polarity widths. Dotted line is the intensity with vertical polarity boundaries. Solid line is the intensity with tilted (53°) polarity boundaries.

CONCLUSION

We constructed new Jurassic GPTS models with new deep-tow magnetic profile and absolute age data from Hole 801C complementing previous study by Sager *et al.* (1998). Total 1200 km of new magnetic profile mostly showing good correlation even among small anomalies except within the LAZ.

In this study, most surveyed anomalies appear strongly linear except for those in the LAZ. Within the LAZ, a zone of low amplitude, difficult-to correlate anomalies, the question of whether the smallest anomalies mapped in previous JQZ studies are correlatable remains unresolved. Perhaps, only one new line may not drastically improve the correlation between the anomalies in this study and that of Sager *et al.* (1998). Nevertheless, upward continuation models made it possible to make nearly one-to-one correlation between old and new anomalies. In terms of difference of correlatability in the LAZ anomalies from other survey areas, the difference suggests either anomalous behavior of the paleomagnetic field or changes in tectonic setting.

In our GPTS modeling, it is impossible to determine which small anomalies represent real polarity reversals and which are intensity fluctuations. The deep-tow GPTS model shows high reversal rate of 12 rev/ Myr due to an assumption of that every small anomaly results from a polarity anomaly. In contrast, a mid-water model, with a reversal rate of 4 rev/ Myr, likely underestimates the number of polarity. Although the uncertainty of correlations in the LAZ (M38-M41) remains, based on overall anomaly correlations the GPTS was extended until 169.4 Ma.

Supporting the assumption that small anomalies in our deep-tow data represent field reversals, logging and paleomagnetic data from Hole 801C and Jurassic continental magnetostratigraphy were investigated. Apparently, high reversal rates inferred from logging data of 60 rev/ Myr calculated by Tivey *et al.* (2005) seems to be an overestimation. This rate is a factor of 5 higher than our GPTS model and is unrealistic value compared to possible predicted reversal rates. However, the reversal rates may vary due to how we interpret lithological boundaries and their ages in the basalt section of Hole 801C. As a reference, the data from Hole 801C suggest that existence of very high reversal rates so that most of small anomalies on our profiles were attributed to actual magnetic reversals.

Changes in anomaly amplitudes on the deep-tow profiles, particularly around the LAZ, may give clues about the origin of the JQZ. The amplitude changes were attributed to : (1) long-term changes both in the crustal magnetization and in Earth's magnetic dipole field, and (2) overlapping of intensity lows because of interference of rapid magnetic field reversals, (3) closely-spaced reversals in the oceanic crust, and (4) changes in Pacific Jurassic tectonics for the changes around the LAZ.

REFERENCES

- Abrams, L. J., R. L. Larson, T. H. Shipley, and Y. Lancelot, (1993) Cretaceous volcanic sequences and Jurassic oceanic crust in the east Mariana and Pigafetta basins of the western Pacific, in *The Mesozoic Pacific: Geology, Tectonics, and Volcanism*, Pringle, M. S., W. W. Sager, W. V. Sliter, and S. Stein, Monograph 77, pp.77-101, American Geophysical Union, Washington D.C.
- Acton, G., G. Guyodo, and S. Brachfeld, (2005) The nature of a cryptochron from a paleomagnetic study of Chron C4r.2r recorded in sediments off the Antarctic Peninsula, *Phys. Earth Planet. Inter.*, submitted.
- Barrett, D. L., and C. E. Keen, (1976) Mesozoic magnetic lineations, the magnetic quiet zone, and sea floor spreading in the northwest Atlantic, *J. Geophys. Res.*, 81, 4875-4884.
- Biggin, A. J., and D. N. Thomas, (2003) Analysis of long-term variations in the geomagnetic poloidal field intensity and evaluation of their relationship with global geodynamics, *Geophys. J. Int.*, 152, 392-415.
- Bowers, N. E., S. C. Cande, J. S. Gee, A. Hildebrand, and R. L. Parker, (2001) Fluctuations of the paleomagnetic field during Chron C5 as recorded in near-bottom marine magnetic anomaly data, *J. Geophys. Res.*, 26379-26396.
- Bowles, J., L. Tauxe, J. Gee, D. McMillan, and S. Cande, (2003) Source of tiny wiggles in Chron C5: A comparison of sedimentary relative intensity and marine magnetic anomalies, *Geochem. Geophys. Geosyst.*, 4(6), 10.1029/2002GC000489.
- Bryant, W. R., and R. H. Bennett, Origin, (1988) Physical and mineralogical nature of red clays: The Pacific Ocean basin as a model, *Geo-Marine. Lett.*, 8, 189-249.
- Cande, S. V., J. L. LaBrecque, and R. L. Larson, (1978) Magnetic anomalies in the Pacific Jurassic Quiet Zone, *Earth Planet. Sci. Lett.*, 41, 434-440.
- Cande, S. V., and D. V. Kent, (1992a) A new geomagnetic polarity time scale for the late Cretaceous and Cenozoic, *J. Geophys. Res.*, 97, 13917-13951
- Cande, S. V., and D. V. Kent, (1992b) Ultrahigh resolution marine magnetic anomaly profiles: A record of continuous paleointensity variations?, *J. Geophys. Res.*, 97, 15075-15083.
- Cande, S. V., and D. V. Kent, (1995) Revised calibration of the geomagnetic polarity timescale for the late Cretaceous and Cenozoic, *J. Geophys. Res.*, 100, 6093-6095.

- Channel. J. E. T., E. Erba, M. Nakanishi, and K. Tamaki, (1995) Late Jurassic- Early Cretaceous time scales and oceanic magnetic anomaly block models. in *Geochronology. Time Scales. And Global Stratigraphic Correlation. SEPM Spec. Publ.*, vol. 54, pp. 51-63, Soc. Sediment. Geol. Tulsa, Okla.
- Denham, C. M., and H. Schouten, (1979) On the likelihood of mixed polarity in oceanic basement drill cores, in *DSDP Results in the Atlantic Ocean: Ocean Crust, Maurice Ewing Symp.*, edited by M. Talwani, C. G. A. Harrison, D. E. Hayes, 2, pp.160-165, AGU, Washington. D. C.
- Gradstein, F. M., F. Agterberg, J. G. Ogg, J. Hardenbol, P. van Veen, J. Thierry, and Z. Huang, A Triassic, (1995) Jurassic, Jurassic and Cretaceous time scale, in *Geochronology. Time Scales. And Global Stratigraphic Correlation. SEPM Spec. Publ.*, vol. 54, pp. 95-126, Soc. Sediment. Geol. Tulsa, Okla.
- Handschoumacher, D. W., W. W. Sager, T. W. C. Hilde, and D. R. Bracey, (1988) Pre-Cretaceous tectonic evolution of the Pacific plate and extension of the geomagnetic polarity reversal timescale with implications for the origin of the Jurassic “Quiet Zone,” *Tectonophysics*, 155, 365-380.
- Hayes, D. E., and P. D. Rabinowitz, (1975) Mesozoic magnetic lineations and the magnetic quiet zone off northwest Africa, *Earth Planet. Sci. Lett.*, 28, 105-115.
- Heller, R., R. T. Merrill, and P. L. McFadden, (2003) The variation of Earth’s magnetic field with time, *Phys. Earth Palnet. Int.*, 131, 237-249.
- Helsley, C. E., and M. B. Steiner, (1969) Evidence for long intervals of normal polarity during the Cretaceous period, *Earth Planet. Sci. Lett.*, 5, 325-332.
- Johnson, H. P., and R. T. Merrill, (1987) A direct test of the Vine-Matthews hypothesis, *Earth Planet. Sci. Lett.*, 40, 263-269.
- Johnson, H. P., and J. E. Pariso, (1993) Variations in oceanic crustal magnetization: Systematic changes in the last 160 million years, *J.Geophys. Res.*, 98, 435-445.
- Koppers, A. A. P., H. Staudigel, and R. A. Duncan, (2003a) High-resolution $^{40}\text{Ar}/^{39}\text{Ar}$ dating for the oldest oceanic basement basalts in the western Pacific basin, *Geochem. Geophys. Geosys.*, 4, doi10.1029/2003GC000574.
- Koppers, A. A. P., H. Staudigel, M. S. Pringle, and J. R. Wijbrans, (2003b) Short-lived and discontinuous intraplate volcanism in the South Pacific: Hot spots or extensional volcanism?, *Geochem. Geophys. Geosys.*, 4, doi 10.1029/2003GC000533.

Kristjansson, L., (1995) New paleomagnetic results from Icelandic Neogene lavas, *Geophys. J. Int.*, 121, 435-443.

Lancelot, T., R. L. Larson and Shipboard Scientific Party, (1990) *Proc. ODP. Proc. Ocean Drill. Prog., Init. Rep.*, Vol. 129, 91-170, Ocean Drill. Prog., College Station, Tex.

Lanci, L., and W. Lowrie, (1997) Magnetostratigraphic evidence that ‘tiny wiggles’ in the oceanic magnetic anomaly record represent geomagnetic paleointensity variations, *Earth Planet. Sci. Lett.*, 148, 581-592.

Larson, R. L., and C. G. Chase, (1972) Late Mesozoic evolution of the western Pacific Ocean, *Geol. Soc. Am. Bull.*, 83, 3627-3644.

Larson, R. L., and W. C. Pitman III, (1972) World-wide correlation of Mesozoic magnetic anomalies and its implications, *Geol. Soc. Am. Bull.*, 83, 3645-3662.

Larson, R. L., and T. W. C. Hilde, (1975) A revised time scale of magnetic reversals for the Early Cretaceous and late Jurassic, *J. Geophys. Res.*, 80, 2586-2594.

Larson, R. L., and S. O. Schlanger, (1981) Geological evolution of the Nauru basin, and regional implications, Deep Sea Drilling Project Leg 61. In Larson, R. L., Schlanger, S. O., et al., *Init. Repts. DSDP*, 61: Washington (U. S. Govt. Printing Office), 533-548.

Larson, R. L. and W. W. Sager, (1992) Skewness of magnetic anomalies M0 to M29 in the northwestern Pacific, *Proc. Ocean Drill. Prog., Sci. Res.*, 129, 471-481.

Larson, R. L., M. B. Steiner, E. Erba, and Y. Lancelot, (1992) Paleolatitudes and tectonic reconstructions of the oldest portion of the Pacific plate: a comparative study, *Proc. Ocean Drill. Prog., Sci. Res.*, 129, 615-631.

Ludden, J., (1992) Radiometric age determinations for basement from Site 765 and 766, Argo abyssal plain and north western Australia, *Proc. Ocean Drill. Prog., Sci. Results.*, 123, 557-559.

MacFadden, P. L., and R. T. Merrill, (1993) Inhibition and geomagnetic field reversals., *J. Geophys. Res.*, 98, 6189-6199

Marzocchi, W., (1997) Missing reversals in the geomagnetic polarity timescale: Their influence on the analysis and in constraining the process that generates geomagnetic reversals, *J. Geophys. Res.*, 102, 5157-5171.

McElhinny, M. W. and R. L. Larson, (2003) Jurassic dipole low defined from land and sea data, *EOS Trans., American Geophysical Union*, 84 (37), 362-366.

- Merrill, R. T. and P. L. McFadden, (1999) Geomagnetic polarity transitions, *Rev. Geophys.*, 37 (2), 201-226.
- Nakanishi, M., K. Tamaki, and K. Kobayashi, (1992) Mesozoic magnetic lineations from late Jurassic to Early Cretaceous in the west central Pacific Ocean, *Geophys. J. Int.*, 109, 701-719.
- Nwogbo, P. O., (1998) Spectral prediction of magnetic source depths from simple numerical models, *Computers & Geosciences*, 24 (9), 847-852.
- Ogg, J. G., and A. Smith, (2004) Mesozoic Geologic Time Scale 2004, *personal communication*, Department of Earth and Atmospheric Sciences, Purdues University, Lafayette, IN.
- Ogg, J. G., M. B. Steiner, F. Oloriz, and J. M. Tevera, (1984) Jurassic magnetostratigraphy, 1. Kimmeridgian-Tithonian of Sierra Gorda and Carcabuey, southern Spain, *Earth planet. Sci. Lett.*, 71, 147- 162.
- Ogg, J. G., M. B. Steiner, J. Wieczorek, and M Hoffman, (1991) Jurassic magnetostratigraphy, 4. Early Callovian through Middle Oxfordian of the Krakow Uplands (Poland), *Earth planet. Sci. Lett.*, 104, 488-504.
- Ogg, J. G., and J. Gutowski, (1995) Oxfordian magnetic polarity time scale, in *Proceedings of the 4th International Congress on Jurassic Stratigraphy and Geology, Geo. Res. Forum* vols. 1-2, edited by A. C. Riccardi, pp. 406-414, Trans-Tec Publ. Ltd., Zurich, Switzerland.
- Olsen, N., T. J. Sabaka, and L. Töffner-Clausen, (2000) Determination of the IGRF 2000 model, *Earth Planets Space*, 52, 1175-1182.
- Onwumechilli, C. A., (1967) Geomagnetic variations in the equatorial zone, in *Physics of Geomagnetic Phenomena*, edited by S. Matsushita and W. H. Campbell. Academic Press, New York, pp. 452-507.
- Pálfy, J., P. L. Smith, and J. K. Mortensen, (2000) A U-Pb and $^{40}\text{Ar}/^{39}\text{Ar}$ time scale for the Jurassic, *Can. J. Earth Sci.*, 37, 923-944.
- Parker, R. L., (1972) The rapid calculation of potential anomalies, *Geophys. J. R. astr. Soc.*, 31, 447-455.
- Parker, R. L., and S. P. Huestis, (1974) The inversion of magnetic anomalies in the presence of topography, *J. Geophys. Res.*, 79, 1587-1593.

- Parker, R. L., (1997) Coherence of signals from magnetometers on parallel paths, *J. Geophys. Res.*, 102, 5111-5117.
- Plank, T., J. N. Ludden, C. Escutia, and Shipboard Scientific Party, (2000) *Proc. ODP., Init. Rep.*, Vol. 185, Ocean Drill. Progr., College Station, Tex.
- Pockalny, R. A., and R. L. Larson, (2002) Implications for crustal accretion at fast spreading ridges from observations in Jurassic oceanic crust in the western Pacific, *Geochem. Geophys. Geosys.*, 4, doi:10.1029/2001GC000274.
- Prévot, M., M. E. Derder, M. McWilliams, and J. Thompson, (1990) Intensity of the Earth's magnetic field: evidence for a Mesozoic dipole low, *Earth Planet. Sci. Lett.*, 97, 129-139.
- Roberts, A. P., and J. C. Lewin-Harris, (2000) Marine magnetic anomalies: evidence that 'tiny wiggles' represent short-period geomagnetic polarity intervals, *Earth planet. Sci. Lett.*, 183, 375-388.
- Roberts, A. P., and M. Winklhofer, (2004) Why are geomagnetic excursions not always recorded in sediments? Constraints from post-depositional remanent magnetization lock-in modeling, *Earth Planet. Sci. Lett.*, 227, 345-359.
- Roser, H. A., C. Steiner, B. Schreckenberger, and M. Block, (2002) Structural development of the Jurassic Magnetic Quiet Zone off Morocco and identification of Middle Jurassic magnetic lineations, *J. Geophys. Res.*, 107, doi:10.1029/2000JB000094.
- Sager, W. W., C. J. Weiss, M. A. Tivey, and H. P. Johnson, (1998) Geomagnetic polarity reversal model of deep-tow profiles from the Pacific Jurassic Quiet Zone, *J. Geophys. Res.*, 103, 5269-5286.
- Schlanger, S. O., H. C. Jenkyns, and I. Premoli-Silva, (1981) Volcanism and vertical tectonics in the Pacific basin related to global transgressions, *Earth Planet. Sci. Lett.*, 52, 435-449.
- Schouten, H., and K. McCamy, (1972) Filtering marine magnetic anomalies, *J. Geophys. Res.*, 77, 7089-7099.
- Schouten, H., and C. R. Denham, (1979) Modeling the oceanic magnetic source layer, in *DSDP Results in the Atlantic Ocean: Ocean Crust, Maurice Ewing Symp.*, edited by M. Talwani, C. G. A. Harrison, D. E. Hayes, 2, pp.151-159, AGU, Washington. D. C.
- Smith, G. M., (1990) The magnetic structure of the marine basement, *Rev. Aquat. Sci.*, 2, 205-227.

Spector, A., and F. S. Grant, (1970) Statistical models for interpreting aeromagnetic data, *Geophysics*, 35, 293-302.

Steiner, M. B., (1980) Inverstigation of the geomagnetic field polarity during the Jurassic, *J. Geophys. Res.*, 85, 3572-3586.

Steiner, M. B., J. G. Ogg, G. Melendez, and L. Sequeiros, (1985) Jurassic magnetostratigraphy, 2. Middle-Late Oxfordian of Aguilon, Iberian Cordillera, northern Spain, *Earth Planet. Sci. Lett.*, 76, 151-166.

Steiner, M. B., J. Ogg, and J. Sandoval, (1987) Jurassic magnetostratigraphy, 3. Bathonian-Bjocian of Carcabuey, Sierra Harana and Campillo de Arenas (Subbetic Cordillera, southern), *Earth Planet. Sci. Lett.*, 82, 357-372.

Steiner, M. B., (2001) Tango in the Mid-Jurassic: 10,000-Yr geomagnetic field reversals, *Eos Trans, AGU Fall meeting Suppl.*, 82(47), GP12A-0205.

Talwani, M., and J. R. Heirtzler, (1964) Computation of magnetic anomalies caused by two-dimensional structures of arbitrary shape, in *Computers in the Mineral Industries*, edited by G.A. Parks, pp. 464-480, Stanford Univ. Press, Stanford, Calif.

Thomas, D. N. and A. J. Biggin, (2003) Does the Mesozoic dipole low really exist?, *Eos, Trans. AGU*, 84, 97, 103-104.

Tivey, M. A., R. L. Larson, R. Pockalny, and H. Schouten, (2005) Downhole magnetic measurements of ODP Hole 801C: Implications for Pacific oceanic crust and magnetic field behavior in the Middle Jurassic., *Geochem. Geophys. Geosys.*, 6, 4, Q04008 doi: 10.1029/2004GC000754.

Valet, J-P., L. Meynadier, and Y. Guyodo, Geomagnetic dipole strength and reversal rate over the past two million years, *Nature*, doi: 10.1038, 2005

Vine, F. J., and D. H. Matthews, (1963) Magnetic anomalies over oceanic ridges, *Nature*, 199, 947-949.

Wallick, B. P., and M. B. Steiner, (1992) Paleomagnetic and rock magnetic properties of Jurassic Quiet Zone basalts, Hole 801C, *Proc. Ocean Drill. Prog., Sci. Results.*, 129, 455-470.

APPENDIX A

Table 1. Deep-tow geomagnetic polarity reversal time scale model

Distance [km]		Age [Ma]		
Young	Old	Young	Old	Chron
14.000	25.750	155.504	155.676	M27r
47.300	58.000	155.989	156.147	M28r
65.125	81.875	156.251	156.495	M28Ar
85.500	91.750	156.548	156.639	M28Br
99.375	105.875	156.751	156.846	M28Cr
111.625	119.500	156.930	157.045	M28Dr
130.625	132.750	157.207	157.238	M29n.1r
137.500	154.375	157.308	157.554	M29r
157.875	162.625	157.605	157.674	M29Ar
171.500	183.000	157.804	157.972	M30r
190.125	192.375	158.076	158.109	M30Ar
203.500	209.375	158.271	158.357	M31n1r
211.375	214.375	158.386	158.429	M31n2r
217.500	221.375	158.476	158.532	M31r
223.000	225.125	158.556	158.587	M32n1r
232.125	235.875	158.689	158.744	M32n2r
238.000	244.000	158.775	158.862	M32r
265.250	274.750	159.173	159.311	M33r
280.375	285.375	159.393	159.466	M33Ar
290.250	298.375	159.538	159.656	M33Br
301.125	304.875	159.696	159.751	M33Cn1r
313.625	328.250	159.879	160.092	M33Cr
333.950	339.050	160.176	160.250	M34n1r
342.250	344.350	160.297	160.328	M34n2r
345.950	349.950	160.351	160.409	M34n3r
352.250	361.550	160.443	160.579	M34Ar
368.050	372.450	160.674	160.738	M34Bn1r
374.450	376.750	160.767	160.801	M34Br
381.450	391.850	160.869	161.021	M35r
399.350	403.350	161.131	161.189	M36n1r
406.475	407.975	161.235	161.256	M36Ar
410.100	420.225	161.287	161.435	M36Br

425.225	434.100	161.508	161.638	N36Cr
451.475	459.725	161.892	162.012	M37n1r
467.700	474.600	162.128	162.229	M37r
484.000	487.500	162.366	162.418	M38n1r
498.000	500.900	162.571	162.613	M38n2r
506.500	514.500	162.695	162.812	M38n3r
530.300	535.200	163.042	163.114	M38n4r
546.300	551.000	163.276	163.345	M38r
563.400	571.500	163.526	163.644	M39n1r
581.600	586.300	163.791	163.859	M39n2r
595.300	604.400	163.991	164.124	M39n3r
614.800	626.900	164.276	164.453	M39n4r
635.600	644.500	164.579	164.709	M39n5r
651.300	658.500	164.809	164.914	M39n6r
663.300	666.500	164.984	165.031	M39n7r
673.400	678.700	165.132	165.209	M39r
681.500	694.100	165.250	165.434	M40n1r
698.800	705.100	165.502	165.594	M40n2r
709.700	725.700	165.662	165.895	M40n3r
727.900	732.800	165.927	165.999	M40r
738.500	751.600	166.082	166.273	M41n1r
756.200	763.500	166.341	166.447	M41n2r
767.700	774.900	166.508	166.613	M41n3r
776.800	784.500	166.641	166.754	M41r
791.800	799.200	166.860	166.968	M42n1r
800.700	803.700	166.990	167.034	M42n2r
807.200	809.900	167.085	167.124	M42n3r
811.600	812.800	167.149	167.167	M42n4r
815.600	817.200	167.208	167.231	M42n5r
818.900	819.900	167.256	167.270	M42n6r
821.900	823.600	167.299	167.325	M42n7r
825.200	828.100	167.348	167.390	M42n8r
832.800	841.500	167.459	167.586	M42n9r
843.100	855.900	167.609	167.796	M42n10r
857.600	864.100	167.821	167.916	M42r
865.200	874.400	167.932	168.066	M43n1r

881.400	887.100	168.168	168.252	M43n2r
890.800	894.000	168.306	168.352	M43n3r
896.300	901.100	168.386	168.456	M43n4r
906.000	911.600	168.528	168.609	M43r
915.000	918.000	168.659	168.703	M44n1r
919.700	923.200	168.728	168.779	M44n2r
925.700	935.300	168.815	168.955	M44n3r
936.500	940.400	168.973	169.030	M44n4r
941.600	946.800	169.047	169.123	M44n5r
947.600	952.400	169.135	169.205	M44n6r
953.100	956.000	169.215	169.258	M44n7r
959.800	961.600	169.313	169.339	M44n8r
964.400	967.000	169.380	169.418	M44r
968.600		169.442		M45-

Table 2. Mid-water geomagnetic polarity reversal time scale model

Distance [km]		Age [Ma]		
Young	Old	Young	Old	Chron
451.475	472.75	161.892	162.202	M37r
480.35	485.15	162.313	162.383	M38n1r
492.313	498.275	162.488	162.575	M38n2r
504.075	512.088	162.659	162.776	M38n3r
528.325	537.325	163.014	163.145	M38n4r
543.475	555.9	163.235	163.416	M38r
562.488	583.488	163.512	163.819	M39n1r
614.888	625.65	164.277	164.434	M39n2r
630.55	641.938	164.506	164.672	M39n3r
647.613	655.013	164.755	164.863	M39n4r
659.433	665.725	164.928	165.02	M39n5r
671.583	677.475	165.105	165.191	M39r
680.883	689.613	165.241	165.368	M40n1r
697.6	703.813	165.485	165.575	M40n2r
706.925	732.183	165.621	165.99	M40r
736.288	739.583	166.05	166.098	M41n1r
742.088	744.683	166.134	166.172	M41n2r
755.288	781.283	166.327	166.707	M41r
790.588	811.283	166.843	167.145	M42n1r
817.688	823.083	167.238	167.317	M42n2r
831.888	833.883	167.446	167.475	M42n3r
850.688	860.583	167.72	167.865	M42r
864.488	880.688	167.922	168.158	M43n1r
888.788	897.483	168.276	168.403	M43n2r
905.288	914.883	168.517	168.657	M43r
931.688	961.183	168.903	169.333	M44n1r
971.288		169.481		M44n2r-?

VITA

Name: Masako Tominaga

Address: 3146 TAMU , Department of Oceanography, Texas A&M University,
College Station, TX 77843-3146

Education: B. E., Waseda University, Tokyo, Japan 2002
Oil Production and Rock Mechanics Lab,
Department of Resource and Environmental Engineering,
School of Science and Engineering

M. S., Texas A&M University, College Station 2005
Department of Oceanography
College of Geosciences